PINSA-A, 64, A, No. 6, November 1998, p. 685-713.
© Printed in India

WAVELET TRANSFORMS AND THEIR APPLICATIONS

LOKENATH DEBNATH

Department of Mathematics, University of Central Florida, Orlando, FL 32816, U.S.A.

(*Received 18 February 1998; Accepted 26 February 1998*)

This paper deals with a brief historial introduction to wavelet transforms and Gabor transforms. Special attention is given to Gabor transforms, continuous wavelet transforms, discrete wavelet theorems and their basic properties. Examples of several wavelets and their Fourier transforms are presented with their graphical representations. This is followed by a discussion of multiresolution analysis, and scaling functions which are used to construct wavelets. Several recent applications of wavelet transform analysis are discussed. These include Weierstrass's and Riemann's everywhere continuous non-differentiable functions, turbulence, galaxies, data compression algorithms, signal and image processing. Many recent references are included in the end to stimulate further study and research on wavelet transforms and their diverse applications.

Key Words: Wavelet Transforms; Gabor Transforms; Multiresolution Analysis; Fourier Transforms; Weierstrass' and Riemann's Non-differentiable Functions; Turbulence; Galaxies in the Universe; Signal and Image Processing; Electromagnetic Wave Phenomena; Electromagnetic and Acoustic Scattering

1 Brief Historical Introduction

The concept of "wavelets" or "ondelettes" started to appear in the literature only in the early 1980s. This new concept can be viewed as a synthesis of various ideas which originated from different disciplines including mathematics (Calderón-Zygmund operators and Littlewood-Paley theory), physics (coherent states formalism in quantum mechanics and renormalization group) and engineering (quadratic mirror filters, sideband coding in signal processing, and pyramidal algorithms in image processing). In 1982, Jean Morlet[1,2], a French geophysical engineer, first introduced the idea of wavelet transform as a new mathematical tool for seismic signal analysis. It was Alex Grossmann, a French theoretical physicist, who quickly recognized the importance of the Morlet wavelet transform which is something similar to coherent states formalism in quantum mechanics, and developed an exact inversion formula for the wavelet transform. Unlike the Weyl-Heisenberg coherent states, the above coherent states arise from translations and dilations of a single function. They are often called *affine coherent states* because they are associated with an affine group (or '$ax+b$' group). The joint venture of Grossmann and Morlet[3] led to a detailed mathematical study of the continuous wavelet transforms and their various applications. It has become clear from their work that, analogous to the Fourier expansions, the wavelet theory has provided a new method for decomposing a function or signal.

In many applications, especially in the time-frequency analysis of a signal, the standard Fourier transform analysis is not adequate because the Fourier transform of the signal does not contain any local information. This is probably the major weakness of the Fourier transform analysis since it neglects the idea of frequencies changing with time or, equivalently, the notion of finding the frequency spectrum of a signal locally in time. In order to eliminate this weakness, in 1946 Dennis Gabor[4], a Hungarian-British physicist and engineer, first introduced the *Windowed-Fourier transform* (or the *short-time Fourier transform*) or more appropriately the *Gabor transform* by using a Gaussian distribution function as the window function. The idea is to use a window function in order to localize the Fourier transform, and then shift the window to another position, and so on. The remarkable feature of the Gabor transform is

the local aspect of the Fourier transform analysis with time resolution equal to the size of the window. In fact, it deals with a discrete set of coefficients which allows efficient numerical computation of those coefficients. However, the Gabor wavelets suffer from some serious algorithmic difficulties which have successfully been resolved by Henrique Malvar[5,6]. Malvar introduced new wavelets which are now known as the Malvar wavelets and fall within the general framework of window Fourier analysis. From an algorithmic point of view, the *Malvar wavelets* are much more effective and superior to other wavelets including Gabor wavelets and Morlet-Grossmann wavelets.

Yves Meyer[7], a French mathematician, recognized immediately the deep connection between the Calderón formula in harmonic analysis and the new algorithm discovered by Morlet and Grossmann. Using the knowledge of the Calderón-Zygmund operators and the Littlewood-Paley theory, Meyer was able to give a mathematical foundation for wavelet theory. The next major achievement of wavelet analysis was due to Daubechies *et al.*[8], who suggested a new construction of a 'painless' non-orthogonal wavelet expansion. During 1985-86, further work of Meyer and Lemarié[9] on the first construction of a smooth orthonormal wavelet basis on R and R^N marked the beginning of their famous contributions to the wavelet theory. At the same time, Stéphans Mallat recognized that some quadratic mirror filters play an important role for the construction of orthogonal wavelet bases generalizing the Haar system. Meyer[7] and Mallat[10] realized that the orthogonal wavelet bases could be constructed systematically from a general formalism. Their collaboration culminated with the remarkable discovery by Mallat of a new formalism[11,12] which is the so called multiresolution analysis. It was also Mallat[13] who constructed the wavelet decomposition and reconstruction algorithms using the multiresolution analysis. Mallat's brilliant work was the major source of many new developments in wavelets. A few months later, Battle[14] and Lemarié[15] independently proposed the construction of spline orthogonal wavelets with exponential decay. While reviewing two books on wavelets in 1993, Meyer[16] states: "Wavelets are without doubt an exciting and intuitive concept. The concept brings with it a new way of thinking, which is absolutely essential and was entirely missing in previously existing algorithms."

Inspired by the work of Meyer, Ingrid Daubechies[17] made a new remarkable contribution to wavelet theory by constructing families of compactly supported orthonormal wavelets with some degree of smoothness. Daubechies[17] paper had a tremendous positive impact on the study of wavelets and their diverse applications. This work significantly explained the connection between the continuous wavelets on R, and the discrete wavelets on Z or Z_N, where the latter has become useful for digital signal analysis. The idea of frames was introduced by Duffin and Schaeffer[18] and subsequently studied in some detail by Daubechies[19,20]. In spite of tremendous success, experts in wavelet theory recognized that it is difficult to construct wavelets that are symmetric, orthogonal and compactly supported. In order to overcome this difficulty, Cohen *et al.*[21,22] studied bi-orthogonal wavelets in some detail. Chui and Wang[23,24] introduced compactly supported spline wavelets, and semi-orthogonal wavelet analysis. On the other hand, Beylkin *et al.*[25] have successfully applied the multiresolution analysis generated by a completely orthogonal scaling function to study a wide variety of integral operators on $L^2(R)$ by a matrix in a wavelet basis. This work culminated with the remarkable discovery of new algorithms in numerical analysis. Consequently, some significant progress has been made in boundary element methods, finite element methods, and numerical solutions of partial differential equations using wavelet analysis.

As a natural extension of wavelet analysis, Coifman *et al.*[26a,b] discovered wavelet packets which can be used to design efficient schemes for the representation and compression of acoustic signals and images. This led them to the construction of a library of orthogonal bases by extending the method of multiresolution decomposition and using the quadratic mirror filters. Recently, there have also been significant applications of wavelet analysis to a wide variety of problems in many diverse fields including mathematics, physics, medicine, computer science, and engineering.

We close this brief historical introduction (*see* Debnath[27,28] by citing some of the applications

which include addressing problems in signal processing, computer vision, seismology, turbulence, computer graphics, image processing, structures of the galaxies and the Universe, digital communication, pattern recognition, approximation theory, quantum optics, biomedical engineering, sampling theory, matrix theory, operator theory, differential equations, numerical analysis, statistics and multiscale segmentation of well logs, natural scenes and mammalian visual systems. Wavelets allow complex information such as music, speech, images, patterns, etc., to be decomposed into elementary form, called building blocks (wavelets). The information is subsequently reconstructed with high precision. In order to describe the present state of wavelet research, Meyer[16] wrote as follows:

"*Today the boundaries between mathematics and signal and image processing have faded, and mathematics has benefited from the rediscovery of wavelets by experts from other disciplines. The detour through signal and image processing was the most direct path leading from Haar basis to Daubechies's wavelets.*"

2 Gabor Transforms and their Basic Properties

Time-frequency analysis has always been challenging in signal processing. In the study of signals represented by a function $f(t)$ (in the multi-dimensional case, $f(t)$ represents an image or a video signal), the idea of frequency analysis can only be local in time. Signals cannot be represented any longer as a superposition of sinusoidal waves of infinite duration, but as a superposition of waves of short duration (or wavelets).

The Fourier transform of a signal or function f is usually defined by Debnath[29].

$$\hat{f}(\omega) = \frac{1}{\sqrt{2\pi}} \int_{-\infty}^{\infty} f(t) e^{-i\omega t} dt. \qquad \ldots (1)$$

One of the remarkable features of this transform is that the integration of the signal is performed over the whole real line R so that every point of R contributes to the analysis of $\hat{f}(\omega)$. So it is difficult to recover local information of f from $\hat{f}$ where the inversion or reconstruction formula is given by

$$f(t) = \frac{1}{\sqrt{2\pi}} \int_{-\infty}^{\infty} \hat{f}(\omega) e^{i\omega t} d\omega. \qquad \ldots (2)$$

The integrand $\hat{f}(\omega)e^{i\omega t}$ has the same modulus $|\hat{f}(\omega)e^{i\omega t}| = |\hat{f}(\omega)|$ for all t, but the local information is contained in the phase. If f vanishes in the neighbourhood of a point $t=t_0$, but it may have some singularities far away from t_0; $|\hat{f}(\omega)|$ remains important for large ω, the flatness of the signal f near t_0 is essentially due to only cancellation between large values of the integrand of opposite signs. This well-known fact leads to highly unstable numerical algorithms. So there is a need to develop the local Fourier analysis so that the numerical instability in near singularities can be controlled instead of spreading over the whole real line. In the case of frequency-modulated signals, the idea of local frequency plays an important role and hence the study of local Fourier transforms becomes important.

In order to determine local information in the Fourier transform analysis, it is necessary to use an analyzing function ψ which has localization properties both in frequency (around some mean frequency (ω_ψ) and in time (around some mean time t_ψ) domains. Such a function ψ is called a wavelet which must be wave of finite duration. In view of the Parseval relation for the Fourier transform

$$(f, \psi) = (\hat{f}, \hat{\psi}), \qquad \ldots (3)$$

where f, $\psi \in L^2(R)$ and (f, ψ) is the inner product in $L^2(R)$. Physically, (f, ψ) can be treated as the average information of f in the vicinity of t_ψ and $(\hat{f}, \hat{\psi})$ is the average information of $\hat{f}$ in the neighbourhood of ω_ψ. A measurement of the resolution of the analyzing function ψ in time or frequency domain is given by the quadratic deviations

$$\Delta\tau_\psi = \left[\int_{-\infty}^{\infty} |t - t_\psi|^2 |\psi(t)|^2 \frac{dt}{\|\psi\|_2^2} \right]^{\frac{1}{2}} \qquad \ldots (4)$$

and

$$\Delta\omega_\psi = \left[\int_{-\infty}^{\infty} |\omega - \omega_\psi|^2 |\hat{\psi}(\omega)|^2 \frac{d\omega}{\|\psi\|_2^2} \right]^{\frac{1}{2}} \qquad \ldots (5)$$

and the joint resolution is given by the product $(\Delta t_\psi)(\Delta\omega_\psi)$. According to Heisenberg's inequality, the joint resolution of ψ cannot be arbitrarily small. More precisely, if $\psi\in L^2(R)$, then $(\Delta t_\psi)(\Delta\omega_\psi)\geq\frac{1}{2}$ and the minimum value of this product is $\frac{1}{2}$ only for Gaussian functions. In other words, there is a strong limitation of a time-frequency analysis in the sense that the product of a time Duration (Δt_ψ) and frequency dispersion $(\Delta\omega_\psi)$ cannot be arbitrarily small. In fact, this product is governed by the Heisenberg uncertainty principle.

In order to incorporate both time and frequency localization properties in one single transform function, Dennis Gabor[4], a Hungarian-British physicist and engineer who won the Nobel Prize for Physics in 1971, first introduced the *windowed Fourier transform* (or the *Gabor transform*) by using a Gaussian distribution function as a window function. His major idea was to use a time-localization window function $g_a(t-b)$ for extracting local information from the Fourier transform of a signal, where the parameter a measures the width of the window, and the parameter b is used to translate the window in order to cover the whole time domain. The idea is to use this window function in order to localize the Fourier transform, then shift the window to another position, and so on. The remarkable property of the Gabor transform is the local aspect of the Fourier transform with time resolution equal to the size of the window. In fact, Gabor[4] used $g_{\nu,t}(\tau)=g(\tau-t)\times\exp(i\nu\tau)$ as the window function by translating and modulating a function $g(\tau)=\pi^{-1/4}\exp(-\frac{1}{2}\tau^2)$, which is the so called *canonical coherent states*. *The continuous Gabor transform* (*Windowed Fourier transform*) of f with respect to g denoted by

$\tilde{f}_g(\nu,t)$ is defined as

$$\mathcal{G}[f](\nu,t)=\tilde{f}_g(\nu,t)=\frac{1}{\sqrt{2\pi}}\int_{-\infty}^{\infty}f(\tau)\bar{g}(\tau-t)e^{i\nu\tau}d\tau$$

$$=\frac{1}{\sqrt{2\pi}}(f,\bar{g}_{\nu,t}), \qquad \ldots(6)$$

where $f,\ g\in L^2(R)$ with the inner product $(f,\ g)$. Clearly, the Gabor transform $\tilde{f}_g(\nu,t)$ of a given signal f depends on both the frequency ν and time t. For any fixed t, $\tilde{f}_g(\nu,t)$ represents the frequency distribution at time t. Usually, only the values $f(\tau)$ for $\tau\leq t$ can be used in computing $\tilde{f}_g(\nu,t)$. With a system of finite memory, there exists a time interval $T>0$ such that only the values $f(\tau)$ for $\tau\geq t-T$ can affect the output at time t. Thus $\tilde{f}_g(\nu,t)$ depends only on $f(\tau)$ for $t-T\leq\tau\leq t$. Mathematically, if $g_{\nu,t}(\tau)$ vanishes outside $[-T,\ 0]$ such that supp $g\subset[-T,\ 0]$ the window function $g_{\nu,t}$ can be used to localize signals in time. For any $t\in R$, we can define $f_t(\tau)=g(\tau-t)f(\tau)$ so that supp $f_t\subset[t-T,\ t]$. So f_t can be regarded as a localized version of f that depends only on the values $f(\tau)$ in $t-T\leq\tau\leq t$. If g is continuous, then the values $f_t(\tau)$ with $\tau\approx t-\tau$ and $\tau\approx t$ are small. This means that the localization is smooth and this particular feature plays an important role in signal processing.

In practical applications, f and g represent signals with finite energy. In quantum mechanics, $\tilde{f}_g(\omega,t)$ is referred to as the *canonical coherent state representation* of f. The term 'coherent states' was first used by Glauber[30] in quantum optics.

The following are immediate consequences of eq. 1.

For a fixed t

$$\mathcal{G}[f](\omega,t)=\tilde{f}_g(\nu,t)=\mathcal{F}\{f_t(\tau)\}=\hat{f}_t(\nu), \qquad \ldots(7)$$

where $\mathcal{F}$ is the Fourier transformation of $f(\tau)$ defined by

$$\hat{f}(\omega)=\mathcal{F}\{f(\tau)\}=\frac{1}{\sqrt{2\pi}}\int_{-\infty}^{\infty}e^{-i\omega\tau}f(\tau)d\tau$$

and $f_t(\tau)=f(\tau)\,g(\tau-t)$.

In view of Parseval's formula for the Fourier transform, (eq. 6) becomes

$$\tilde{f}_g(\nu,t)=\frac{1}{\sqrt{2\pi}}\left(\hat{f},\hat{\bar{g}}_{\nu,t}\right),\ \hat{f}(\nu)=\mathcal{F}\{f(\tau)\}$$

$$=\frac{1}{\sqrt{2\pi}}\left(\hat{f},e^{it(\omega-\nu)}\bar{\hat{g}}(\omega-\nu)\right)$$

$$=\frac{1}{\sqrt{2\pi}}e^{i\nu t}\int_{-\infty}^{\infty}\hat{f}(\omega)e^{-i\omega\nu}\hat{g}(\omega-\nu)d\nu. \qquad \ldots(8)$$

Except for the factor $\exp(i\nu t)$, result eq. (8) is

almost identical with eq. (6), but the time variable τ is replaced by the frequency variable ν and the time window function $g(\tau-t)$ replaced by the frequency window function $\hat{g}(\omega-\nu)$. The extra factor $\exp(i\nu t)$ in eq. (8) is associated with the Weyl commutation relations of the Weyl-Heisenberg group which describes translations in time and frequency. If the window is well localized in frequency as well as in time, that is, if $\hat{g}(\omega)$ is small outside a small frequency band in addition to $g(t)$ being small outside a small time interval, then eq. (8) reveals that the Gabor transform gives a local time-frequency analysis of the signal f in the sense that it provides accurate information of f simultaneously in both time and frequency domains. However, all functions, including window functions, satisfy the Heisenberg uncertainty principle which states that time and frequency of a signal cannot be measured precisely and simultaneously. In other words, the joint resolution $(\Delta t_\psi)(\Delta\omega_\psi)$ of a signal cannot be arbitrarily small, and has always greater than the minimum value $\frac{1}{2}$ which is attained only for Gaussian windows $g(t)=\exp(-at^2)$.

For a fixed ν

$$\mathcal{G}[f(\tau)](\nu,t)=e^{-i\nu t}[f(t)*e^{i\nu t}g(-t)] \quad \ldots(9)$$

where the convolution of f and g is defined by

$$f(t)*g(t)=\frac{1}{\sqrt{2\pi}}\int_{-\infty}^{\infty}f(\tau)g(t-\tau)d\tau.$$

If $g(\tau)=\exp(-\frac{1}{4}\tau^2)$, then

$$\mathcal{G}[f(\tau)](\nu,t)=\sqrt{2}e^{-\nu^2+it\nu}(Wf)(t+2i\nu), \quad \ldots(10)$$

where W represents the Weierstrass transformation of $f(x)$ defined by

$$W[f(x)]=\frac{1}{2\sqrt{\pi}}\int_{-\infty}^{\infty}f(x)\exp\left[-\frac{1}{4}(t-x)^2\right]dx.$$

The following theorem gives several basic properties of the continuous Gabor transform.

Theorem 2.1 If $\mathcal{G}$ represents the continuous Gabor transformation, defined by eq. (1), then

(i) (*Linearity*): $\mathcal{G}$ is a linear transformation, that is:

$$\mathcal{G}[af_1+bf_2](\omega,t)=a\mathcal{G}[f_1](\nu,t)+b\mathcal{G}[f_2](\nu,t), \quad \ldots(11)$$

where a and b are constants.

(ii) (*Translation*):

$$\mathcal{G}[f(\tau-a)](\nu,t)=e^{ia\nu}\mathcal{G}[f(\tau)](\nu,t-a), \quad \ldots(12)$$

(iii) (*Modulation*):

$$\mathcal{G}[e^{ia\tau}f(\tau)](\nu,t)=\mathcal{G}[f(\tau)](\nu+a,t), \quad \ldots(13)$$

(iv) (*Conjugation*): If the window function g is real, then

$$\mathcal{G}[\bar{f}(\tau)](\nu,t)=\bar{\mathcal{G}}[f(t)](-\nu,t). \quad \ldots(14)$$

(v) (*Parseval's formula*): If the window function $g\in L^2(R)$ with $\tilde{f}_g(\nu,t)$ and $\tilde{h}_g(\nu,t)$ as their Gabor transforms respectively, then Parseval's formula of f, h for the Gabor transform is given by

$$(\tilde{f},\tilde{h})=\|g\|^2(f,h), \quad \ldots(15)$$

where

$$(\tilde{f},\tilde{h})=(\tilde{f},\tilde{h})_{L^2(R^2)}=\int_{-\infty}^{\infty}\int_{-\infty}^{\infty}\tilde{f}(\nu,t)\bar{\tilde{h}}(\nu,t)d\nu dt. \quad \ldots(16)$$

In particular, if $\|g\|=1$, then the Gabor transformation is an isometry from $L^2(R)$ into $L^2(\mathbb{R}^2)$.

Proofs of (i)-(iii) are straightforward consequences of the definition and hence are left to the reader. We give a proof of (iv). To prove eq. (15) we note that, for a fixed t, $\tilde{f}(\omega,t)$ is the Fourier transform of the function $f(\tau)g_t(\tau)$ where $g_t(\tau)=g(\tau-t)$, that is, $\tilde{f}(\nu,t)=\mathcal{F}\{(fg_t)\}$. Thus, Parseval's formula for the Fourier transform gives

$$\int_{-\infty}^{\infty}\tilde{f}(\nu,t)\bar{\tilde{h}}(\nu,t)d\nu=(\mathcal{F}(fg_t),\mathcal{F}(hg_t))=(fg_t,hg_t)$$

$$=\int_{-\infty}^{\infty}f(\tau)\bar{h}(\tau)|g(\tau-t)|^2d\tau.$$

Integrating this result with respect to t from $-\infty$ to ∞ gives

$$(\tilde{f},\tilde{h})=\int_{-\infty}^{\infty}f(\tau)\tilde{h}(\tau)d\tau\int_{-\infty}^{\infty}|g(\tau-t)|^2dt$$

$$=\int_{-\infty}^{\infty}f(\tau)\tilde{h}(\tau)d\tau\int_{-\infty}^{\infty}|g(x)|^2dx,\ \tau-t=x$$

$$=\|g\|^2(f,h).$$

This proves the result. If $\|g\|=1$, then eq. (15) shows the isometry.

Theorem 2.2 *(Inversion Formula).* If $\mathcal{G}[f](\nu,t) = \tilde{f}_g(\nu,t)$, then

$$f(\tau) = \frac{1}{\sqrt{2\pi}} \frac{1}{\|g\|^2} \int_{-\infty}^{\infty} \int_{-\infty}^{\infty} \tilde{f}_g(\nu,t)\bar{g}(\tau-t)e^{-i\tau\nu}\, d\nu dt. \quad \ldots (17)$$

Proof. It follows from eq. (7) that

$$\tilde{f}_g(\nu,t) = \tilde{f}_t(\nu).$$

Application of the inverse Fourier transform with respect to the variable ν gives

$$g(\tau-t)f(\tau) = f_t(\tau) = \mathcal{F}^{-1}\{\tilde{f}_g(\nu,t)\} = \frac{1}{\sqrt{2\pi}} \int_{-\infty}^{\infty} e^{i\nu\tau} \tilde{f}_g(\nu,t)\, d\nu \quad \ldots (18)$$

Multiplying this result by $\bar{g}(\tau-t)$ and integrating with respect to t yields

$$f(\tau) \int_{-\infty}^{\infty} |g(\tau-t)|^2 dt = \frac{1}{\sqrt{2\pi}} \int_{-\infty}^{\infty} \int_{-\infty}^{\infty} e^{i\nu\tau} \bar{g}(\tau-t) \times \tilde{f}_g(\nu,t) d\nu. \quad \ldots (19)$$

This proves the result eq. (17).

In terms of the sampling points defined by $\omega = m\omega_0$ and $t = nt_0$ where m, n are integers and ω_0 and t_0 are positive quantities, the discrete Gabor functions are defined by $g_{m,n}(t) = \exp(im\omega_0 t)g(t-nt_0)$. These functions are called the *Weyl-Heisenberg coherent states* which arise from translations and modulations of the Gabor window function. From a physical point of view, these coherent states are of special interest. They have led to several important applications in quantum mechanics. Subsequently, various other functions have been used as window functions instead of the Gaussian function which was originally introduced by Gabor. The *discrete Gabor transform* is defined by

$$F(m,n) = \int_{-\infty}^{\infty} f(t)\bar{g}_{m,n}(t)dt = (f, g_{m,n}) \quad \ldots (20)$$

The double series $\sum_{m,n=-\infty}^{\infty} F(m,n)g_{m,n}(t)$ is called the *Gabor series* of $f(t)$.

In many applications, it is more convenient, at least from a numerical point of view, to deal with discrete transforms rather than continuous ones. It is of special interest to determine the inverse discrete Gabor transform so that the function $f \in L^2(R)$ can be determined from the formula

$$F(m\omega_0, nt_0) = \frac{1}{\sqrt{2\pi}} \int_{-\infty}^{\infty} f(t)g_{m,n}(t)dt = \frac{1}{\sqrt{2\pi}}(f, \bar{g}_{m,n}) \quad \ldots (21)$$

If the functions $\{g_{m,n}(t)\}$ form an orthonormal basis or, more generally, if they form a frame for $L^2(R)$, then f can be reconstructed by the formula

$$f(t) = \sum_{m,n=-\infty}^{\infty} (f, g_{m,n})g^*_{m,n}(t), \quad \ldots (22)$$

where $\{g^*_{m,n}(t)\}$ is called the *dual frame* of $\{g_{m,n}(t)\}$. $\{g_{m,n}(t)\}_{m,n=-\infty}$ is called a *Gabor frame.* The set of sample points $\{(m\omega_0, nt_0)\}$, when $m, n \in Z$ is called a *Gabor lattice.* The Gabor discrete transform deals with a discrete set of coefficients which allows efficient numerical computation of those coefficients. However, Henrique Malvar[5,6] recognized some serious algorithmic difficulties in the Gabor wavelet analysis. He resolved these difficulties by introducing new wavelets which are now known as the *Malvar wavelets* and fall within the general framework of the window Fourier analysis. From an algorithmic point of view, the Malvar wavelets are much more effective and are superior to Gabor wavelets, and to other wavelets.

Finding the conditions on ω_0, t_0, and g under which the Gabor series of f determines f or converges to it is known as the *Gabor representation problem.* Gabor discussed this problem in the case $\omega_0 t_0 = 2\pi$ and g is a Gaussian function.

The Fourier transform $\hat{g}_{m,n}(\omega)$ of $g_{mn}(t)$, provided that it exists, can be obtained as

$$\hat{g}_{m,n}(\omega) = \exp[int_0(\omega + m\omega_0)]\hat{g}(\omega + m\omega_0). \quad \ldots (23)$$

Thus

$$\|\hat{g}_{m,n}\| = \|\hat{g}_{m,n}\|_2 = \|\hat{g}\|_2. \quad \ldots (24)$$

If g is centered around (0, 0) in the time-frequency domain, that is,

$$\int_{-\infty}^{\infty} t|g(t)|^2 dt = 0 = \int_{-\infty}^{\infty} \omega|g(\omega)|^2 d\omega, \text{ with } \|g\| = 1,$$

then

$$\int_{-\infty}^{\infty} |g_{m,n}(t)|^2 dt = nt_0 \text{ and } \int_{-\infty}^{\infty} \omega |\hat{g}_{m,n}(\omega)|^2 d\omega = -m\omega_0. \quad \ldots (25a,b)$$

In many physical applications, the window function g in eq. (6) is assumed as a bounded function with compact support or of rapid decay as $|t| \to \infty$. In both cases, if $f \in L^1(R)$, $\tilde{f}_g(\nu, t)$ exists almost everywhere in R^2. In practice, f and g represent signals with finite energy and hence f, $g \in L^2(R)$. Thus the Gabor transform $\tilde{f}(\nu, t)$ of f exists whenever $f \in L^2(R)$.

On the other hand, if $f \in L^2(R)$, and $\{g_{m,n}\}$ is a frame in $L^2(R)$, then

$$\sum_{m,n=-\infty}^{\infty} |(f, g_{m,n})|^2 < \infty.$$

This implies that the Gabor series of f converges in $L^2(R)$, but not necessarily to this function f. However, sufficient conditions exist for $\{g_{m,n}\}$ to be a frame in $L^2(R)$ (see Zayed[31]).

It has been indicated earlier that the Gabor representation problem plays an important role in many physical and engineering problems. The following results are associated with these problems:

1. $\{g_{m,n}(t)\}$, $m, n \in Z$ represents a frame if and only if $\{\hat{g}_{m,n}(\omega)\}$ is a frame in $L^2(R)$. This follows from Parseval's formula for the Fourier transform.
2. If $\{g_{m,n}(t)\}$ is the frame generated by g, then its dual frame $\{g^*_{m,n}(t)\}$ is also generated by one function by translation and modulation.
3. If $\{g_{m,n}(t)\}$ is a frame in $L^2(R)$ with frame bounds A and B, then

$$A \le \left(\frac{2\pi}{\omega_0 t_0}\right) \|g\|^2 \le B. \quad \ldots (26)$$

The frame is called a *tight frame* if $A = B = \left(\frac{2\pi}{\omega_0 t_0}\right)\|g\|^2$. In particular, for $\{g_{mn}\}$ to be an orthonormal basis, $\omega_0 t_0 = 2\pi$ provided $\|g\| = 1$.

Finally, if $0 < \omega_0 t_0 < 2\pi$, then it is possible for $\{g_{mn}(t)\}$ to be a frame, provided that the window function g satisfies extra conditions which can be illustrated by the following theorem:

Theorem 2.3. If g and t_0 are such that

$$0 < \inf_{0 \le t < t_0} G(t) \le \sup_{0 \le t \le t_0} G(t) < \infty$$

where $G(t) = \sum_{n=-\infty}^{\infty} |g(t - nt_0)|^2$, and if

$$a(x) = \sup_{0 \le t \le t_0} \sum |g(t - nt_0)||g(t - nt_0 + x)|$$

decays at least as rapidly as $(1+|x|)^{-(1+\varepsilon)}$ as $x \to \infty$ for $\varepsilon > 0$, then there exists $\sigma > 0$ such that $\{g_{m,n}(t)\}$ is a frame whenever $\sigma > \omega_0$.

For the so called critical case $\omega_0 t_0 = 2\pi$, there is a frame of the form $\{g_{m,n}(t)\}$, but g does not have good localization properties either in the time or frequency domain. More precisely, if $\{g_{m,n}(t)\}$ represents a frame in $L^2(R)$, then either

$$\int_{-\infty}^{\infty} t^2 |g(t)|^2 dt = \infty, \text{ or } \int_{-\infty}^{\infty} \omega^2 |\hat{g}(\omega)|^2 d\omega = \infty.$$

However, Gabor considered the Gaussian function which has very good localization properties. In this case, it is not possible to generate a frame, but the associated sequence $\{g_{m,n}(t)\}$ is complete.

For the case $\omega_0 t_0 > 2\pi$, there is no frame of the form $\{g_{m,n}(t)\}$ whatever the choice of g. In fact, $\{g_{m,n}\}$ is not even complete in the sense that there exists $f \in L^2(R)$ such that $(f, g_{m,n}) = 0$ for all m, n with $f \neq 0$.

In contrast to the other two cases, only in the critical case ($\omega_0 t_0 = 2\pi$), there is an orthonormal basis $\{g_{m,n}\}$. It also follows from eq. (26) that for a tight frame with frame bounds equal to unity, $\omega_0 t_0 = 2\pi$.

We close this section by adding a few comments. First, several other window functions have been suggested in signal processing such as regular windows with compact support. Regularity is essential in order to avoid generation of high frequencies in the signal $f(t)g(t - nt_0)$. Second, the Wigner-Ville transform has also been introduced by Ville[32] for the time-frequency analysis of a signal. This transform is defined by

$$W_f(t, \omega) = \int_{-\infty}^{\infty} f\left(t + \frac{\tau}{2}\right) \bar{f}\left(t - \frac{\tau}{2}\right) e^{-i\omega\tau} d\tau \quad \ldots (27)$$

and satisfies the properties

$$\int_{-\infty}^{\infty} W_f(t,\xi)dt = |\hat{f}(\xi)|^2 \text{ and } \int_{-\infty}^{\infty} W_f(t,\xi)\frac{d\xi}{2\pi} = |f(t)|^2 \quad \ldots (28a,b)$$

The Wigner-Ville transform seems to be an effective tool for signals of short duration.

Third, the theory of Gabor transforms has been generalized by Janssen[33a,b] for tempered distributions. Among many important results, he proved that any tempered distribution can be written as

$$\sum_{m,n} c_{m,n}\, g_{m,n}(t), \quad \ldots (29)$$

where g is not necessarily a Gaussian function, but a function $g \in S$ where S is the Schwartz space of generalized function.

Fourth, the n-dimensional Gabor transform of a function f with respect to the window function g can be defined by

$$\mathcal{G}[f](\nu,t) = \tilde{f}_g(\nu,t) = \frac{1}{(2\pi)^{n/2}} \int_{\infty}^{\infty} \cdots \int_{\infty}^{\infty} f(x)\, g(x-t) e^{i(\nu\cdot x)} dx, \quad \ldots (30)$$

where ν, t, $x \in R^n$, $x=(x_1, x_2, \ldots x_n)$, and ν. $x = \nu_1 x_1 + \nu_2 x_2 + \ldots + \nu_n x_n$. Clearly, the Gabor transformation provides a representation of n variables by a function $2n$ variables.

Finally, the Gabor transformation has been found to be very useful in many physical and engineering applications, including signal processing and quantum optics[34].

3 Continuous Wavelet Transforms and Their Basic Properties

Morlet[1,2] modified the Gabor wavelets to study the layering of sediments in a geophysical problem of oil exploration. He recognized certain difficulties of the Gabor wavelets in the sense that the Gabor analyzing functions $g_{\nu,t}(\tau) = e^{i\nu\tau} g(\tau - t)$ oscillates more rapidly as the frequency ν tends to infinity. This leads to significant numerical instability in the computation of the coefficients $(f, g_{\nu,t})$. On the other hand, $g_{\nu,t}$ oscillates very slowly at low frequencies. These difficulties led to a problem of finding a suitable reconstruction formula. In order to resolve these difficulties, Morlet first made an attempt to use analytic signals $f(t) = a(t)\exp\{i\phi(t)\}$ and then introduced the wavelet ψ defined by its Fourier transform

$$\hat{\psi}(\omega) = \omega^2 \exp\left(-\frac{1}{2}\omega^2\right), \quad \omega > 0 \quad \ldots (31)$$

This corresponds to an analytic signal related to the second derivative $(1-t^2)\exp\left(-\frac{1}{2}t^2\right)$ of the Gaussian function $\exp\left(-\frac{1}{2}t^2\right)$. Thus, the Morlet wavelet turned out to be the modulated Gaussian function. In fact, Morlet's ingenious idea was to filter the signal $f(t)$ with the aid of the filters $\hat{\psi}(a^m\omega)$, $m \in Z$ so that

$$f(t) \to f_m(t) = \int_{-\infty}^{\infty} f(t-\tau) a^{-m} \hat{\psi}(a^{-m}\tau) d\tau. \quad \ldots (32)$$

Morlet's analysis showed that the quantity $\sum_{m\in Z} |\hat{\psi}(a^m\omega)|^2$ remained constant for sufficiently small a. Also it led to stable and fast reconstruction algorithms of f from f_m even when $a=2$. Moreover, Morlet suggested sufficiently small mesh sizes so that they allow a good reconstruction algorithm of analytic signals with coefficients

$$c_{mn} = f_m(n2^m) = \left(f(t), 2^{-m}\psi(2^{-m}t - n)\right). \quad \ldots (33)$$

Thus Morlet's remarkable analysis led to the discovery of the wavelet transform which seems to be an efficient and effective time-frequency representation algorithm. The major difference between the Morlet wavelet representation and the Gabor wavelet is that the former has a more and more acute spatial resolution as the frequency gets higher and higher.

Based on the idea of wavelets as a family of functions constructed from translation and dilation of a single function ψ, called the *mother wavelet*, we define *wavelets* by

$$\psi_{a,b}(t) = \frac{1}{\sqrt{|a|}}\psi\left(\frac{t-b}{a}\right), a,b \in R, a \neq 0, \quad \ldots (34)$$

where a is called a *scaling parameter* which measures the degree of compression or scale, and b as *translation parameter* which determines the time location of the wavelet. If $|a|<1$, the wavelet

eq. (34) is the compressed version (smaller support in time-domain) of the mother wavelet and corresponds to mainly higher frequencies. Thus wavelets have time-width adapted to their frequencies. This is the main reason for the success of the Morlet wavelets in signal processing and time-frequency signal analysis. It may be noted that the resolution of wavelets at different scales varies in the time and frequency domains as governed by the Heisenberg uncertainty principle. At large scale, the solution is coarse in the time domain and fine in the frequency domain. As the scale a decreases, the resolution in the time domain becomes finer while that in the frequency domain becomes coarser.

Morlet first called his functions 'wavelets of constant shape' in order to contrast them with the analyzing functions in the short-time Fourier transform which do not have a constant shape. From a group-theoretic point of view, the wavelets $\psi_{a,b}(x)$ are in fact the result of the action of the operators $U(a,b)$ on the function ψ so that

$$[U(a,b)\psi](x)=\frac{1}{\sqrt{|a|}}\psi\left(\frac{x-b}{a}\right) \qquad \ldots (35)$$

These operators are all unitary on the Hilbert space $L^2(R)$ and constitute a representation of the '$ax+b$' group

$$U(a,b)U(c,d)=U(ac,b+ad). \qquad \ldots (36)$$

$$U(1,0)=Id$$

$$U(a,b)^{-1}=U\left(\frac{1}{a},-\frac{b}{a}\right)$$

This group representation is *irreducible*, that is, for any non-zero $f\in L^2(R)$, there exists no non-trivial g orthogonal to all the $U(a,b)f$. In other words, $U(a,b)f$ span the entire space. The multiplication of operators defines the product of pairs (a,b), $(c,d)\in \mathrm{R}/\{0\}\times \mathrm{R}$, that is $(a,b)\circ(c,d)=(ac, b+ad)$. Like the operators $U(a,b)$, the pairs (a,b) together with the operation $\circ$ form a group. The coherent states associated with the $(ax+b)$-group, which are now known as wavelets, were first formulated by Aslaksen and Klauder[35,36]. The success of Morlet's numerical algorithms prompted Grossmann to make a more extensive study of the Morlet wavelet transform which led to the recognition that wavelets $\psi_{a,b}(t)$ correspond to a square integrable representation of the affine group.

We next give formal definitions of a wavelet and a continuous wavelet transform of a function.

Definition 3.1 (*Wavelet*). A *wavelet* is a function $\psi\in L^2(R)$ which satisfies the condition

$$\int_{-\infty}^{\infty}\frac{|\hat{\psi}(\omega)|^2}{|\omega|}d\omega<\infty \qquad \ldots (37)$$

where $\hat{\psi}(\omega)$ is the Fourier transform of $\psi(t)$.

Definition 3.2 (*Continuous Wavelet Transform*). If $\psi\in L^2(R)$, and $\psi_{a,b}(t)$ is given by eq. (34), then the integral transformation W_ψ defined on $L^2(R)$ by

$$W_\psi[f](a,b)=(f,\psi_{a,b})=\int_{-\infty}^{\infty}f(t)\overline{\psi_{a,b}(t)}dt \qquad \ldots (38)$$

is called a *continuous wavelet transform* of $f(t)$.

Note. The kernel $\psi_{a,b}(t)$ in eq. (38) plays the same role as the kernel $\exp(-i\omega t)$ in the Fourier transform. However, unlike the Fourier transformation, the continuous wavelet transform is not

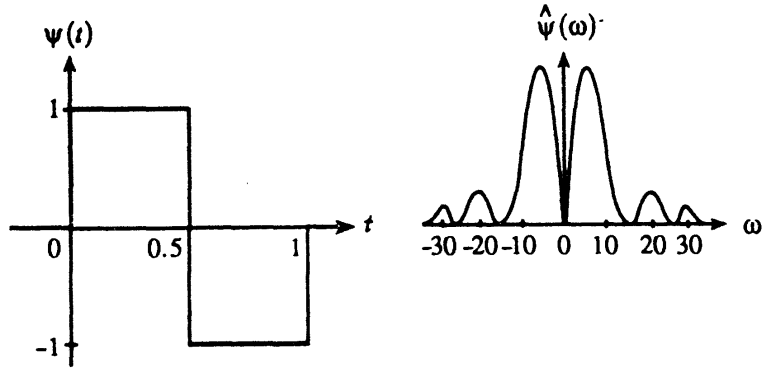

Fig. 1 The Haar wavelet and its Fourier transform

a *single* transform, but any transform obtained in this way. Like the Fourier transformation, the continuous wavelet transformation is linear.

Example 3.1 (*Haar Wavelet*). The Haar wavelet (1910) is one of the classic examples. It is defined by

$$\psi(t)=\begin{cases} 1, & 0\le t<\frac{1}{2} \\ -1, & \frac{1}{2}\le t<1 \\ 0, & \text{otherwise} \end{cases}. \qquad \ldots(39)$$

Its Fourier transform is given by

$$\hat{\psi}(\omega)=\frac{1}{\sqrt{2\pi}}\frac{\sin^2\frac{\omega}{4}}{\left(\frac{\omega}{4}\right)}\exp\left[\frac{i}{2}(\pi-\omega)\right] \qquad \ldots(40a)$$

and

$$\int_{-\infty}^{\infty}\frac{|\hat{\psi}(\omega)|^2}{|\omega|}d\omega=\frac{8}{\pi}\int_{-\infty}^{\infty}\frac{\left|\sin\frac{\omega}{4}\right|^4}{|\omega|^3}d\omega<\infty. \qquad \ldots(40b)$$

Both $\psi(t)$ and $\hat{\psi}(\omega)$ are plotted in Fig. 1.

Theorem 3.1. If ψ is a wavelet and ϕ is bounded integrable function, then the function $\psi*\phi$ (convolution of ψ and ϕ) is a wavelet.

Proof. According to the theory of Fourier transform, $\psi*\phi\in L^2(R)$. Then

$$\int_{-\infty}^{\infty}\frac{|\psi*\phi(\omega)|^2}{|\omega|}d\omega=\int_{-\infty}^{\infty}\frac{|\hat{\psi}(\omega)\hat{\phi}(\omega)|^2}{|\omega|}d\omega$$

$$=\int_{-\infty}^{\infty}\frac{|\hat{\psi}(\omega)|^2}{|\omega|}|\hat{\phi}(\omega)|^2d\omega$$

$$\le\int_{-\infty}^{\infty}\frac{|\hat{\psi}(\omega)|^2}{|\omega|}d\omega\sup|\hat{\phi}(\omega)|^2<\infty.$$

Example 3.2 Using Theorem 3.1, we can easily generate other wavelets. For example, if we take

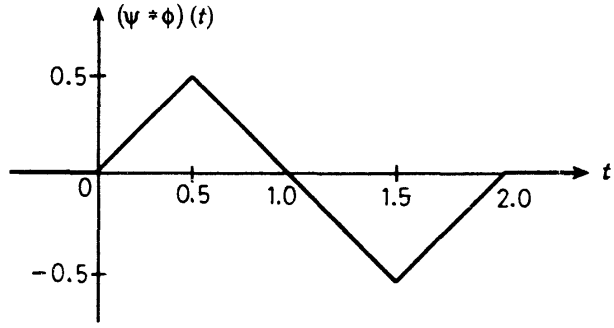

Fig. 2 The wavelet $(\psi*\phi)(t)$.

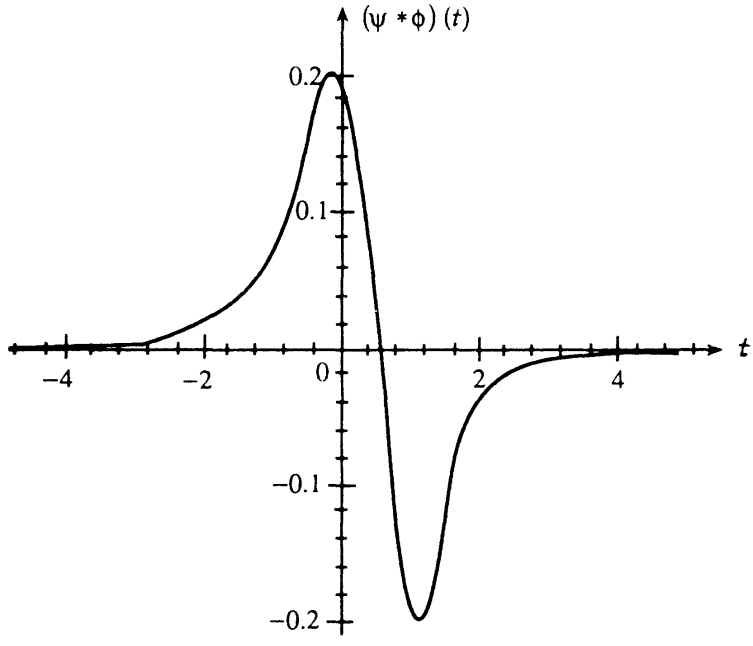

Fig. 3 The wavelet $(\psi*\phi)(t)$.

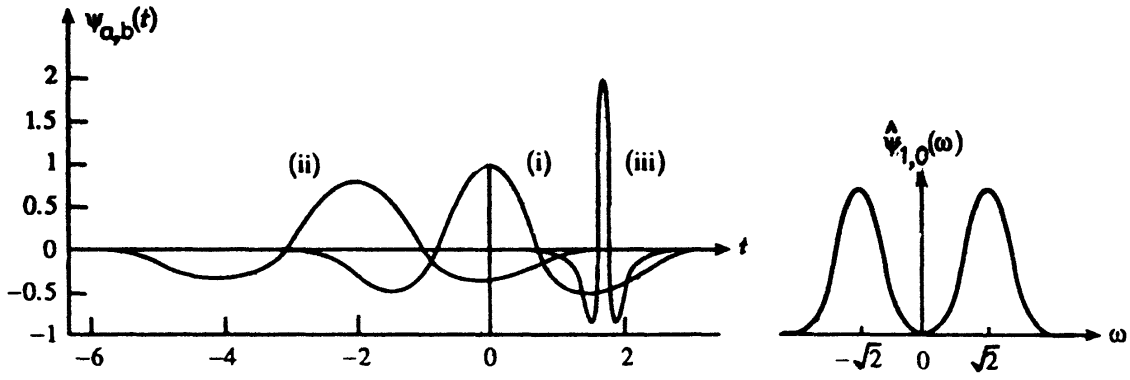

Fig. 4 The Mexican hat wavelet $\psi(t)$ and $\psi_{1,0}(\omega)$.

the Haar wavelet and convolute it with the following function

$$\phi(t)=\begin{Bmatrix}0, & t<0\\ 1, & 0\le t\le 1\\ 0, & t\ge 1\end{Bmatrix}, \qquad \ldots(41)$$

we obtain a simple wavelet as shown in Fig. 2.

Example 3.3 The convolution of the Haar wavelet with $\phi(t)=\exp(-t^2)$ generate a smooth wavelet as shown in Fig. 3.

Example 3.4 (*The Mexican Hat Wavelet*). The Mexican hat wavelet is defined by the second derivative of a Gaussian function as

$$\psi(t)=\left(1-2t^2\right)\exp\left(-t^2\right)=\psi_{1,0}(t) \qquad \ldots(42)$$

$$\hat{\psi}(\omega)=\hat{\psi}_{1,0}(\omega)=\frac{\omega^2}{\sqrt{2\pi}}\exp\left(-\omega^2\right). \qquad \ldots(43)$$

In contrast to the Haar wavelet, the Mexican hat wavelet is a C^{∞}-function. It has two vanishing moments. Two other wavelets $\psi_{\frac{3}{2},-2}(t)$ and $\psi_{\frac{1}{4},\sqrt{2}}(t)$ from the mother wavelet eq. (42) can be obtained. These three wavelet $\psi_{1,0}(t)$, $\psi_{\frac{3}{2},-2}(t)$ and $\psi_{\frac{1}{4},\sqrt{2}}(t)$ are shown in Fig. 4 (i), Fig. 4 (ii) and Fig. 4 (iii) respectively.

Example 3.5 (*Morlet Wavelet*). The Morlet wavelet is defined by

$$\psi(t)=\exp\left(i\omega_0 t-\frac{t^2}{2}\right) \qquad \ldots(44)$$

$$\hat{\psi}(\omega)=\frac{1}{\sqrt{2\pi}}\exp\left[-\frac{1}{2}(\omega-\omega_0)^2\right]. \qquad \ldots(45)$$

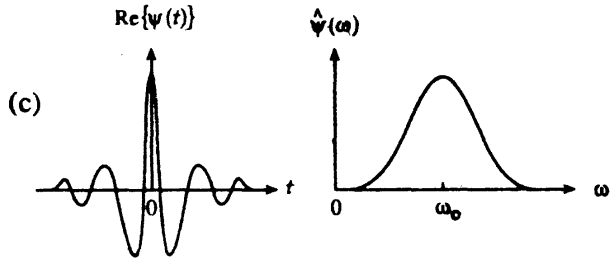

Fig. 5 Graphs of $\psi(t)$ and $\hat{\psi}(\omega)$.

They are plotted in Fig. 5.

The following theorem gives several properties of continuous wavelet transform.

Theorem 3.2 If ψ and ϕ are wavelet and f, g are functions which $\in L^2(R)$, then

(i) (*Linearity*):

$$W_{\psi}(\alpha f+\beta g)(a,b)=\alpha\left(W_{\psi}f\right)(a,b)+\beta\left(W_{\psi}g\right)(a,b), \qquad \ldots(46)$$

where α, β are any scalars.

(ii) (*Translation*):

$$\left(W_{\psi}\left(T_c f\right)\right)(a,b)=\left(W_{\psi}f\right)(a,b-c), \qquad \ldots(47)$$

where T_c is the *translation operator* defined by $T_c f(t)=f(t-c)$.

(iii) (*Dilation*):

$$\left(W_{\psi}\left(D_c f\right)\right)(a,b)=\frac{1}{\sqrt{c}}\left(W_{\psi}^{\cdot}f\right)\left(\frac{a}{c},\frac{b}{c}\right), c>0, \qquad \ldots(48)$$

where D_c is a *dilation operator* defined by $D_c f(t)=\frac{1}{\sqrt{c}}f\left(\frac{t}{c}\right)$, $c>0$.

(iv) (*Symmetry*):

$$\overline{(W_\psi f)(a,b)} = (W_f \psi)\left(\frac{1}{a}, -\frac{b}{a}\right), \quad a \neq 0. \qquad \ldots (49)$$

(v) (*Parity*):

$$(W_{P\psi} Pf)(a,b) = (W_\psi f)(a,-b), \qquad \ldots (50)$$

where P is the *parity operator* defined by $Pf(t)=f(-t)$.

(vi) (*Antilinearity*):

$$(W_{\alpha\psi+\beta\phi} f)(a,b) = \bar{\alpha}(W_\psi f)(a,b) + \bar{\beta}(W_\phi f)(a,b),$$

for any scalars α, β $\ldots (51)$

$$\text{(vii)} \quad (W_{T_c\psi} f)(a,b) = (W_\psi f)(a, b+ca). \qquad \ldots (52)$$

$$\text{(viii)} \quad (W_{D_c\psi} f)(a,b) = \frac{1}{\sqrt{c}}(W_\psi f)(ac, b), \; c>0. \qquad \ldots (53)$$

Proofs are straightforward and are left as exercises.

Theorem 3.3 (*Parseval's Formula for Wavelet Transforms*). If $\psi \in L^2(R)$ so that

$$C_\psi = 2\pi \int_{-\infty}^{\infty} \frac{|\hat{\psi}(\omega)|^2}{|\omega|}\, d\omega < \infty, \qquad \ldots (54)$$

then, for any functions f, $g \in L^2(R)$, we obtain

$$\int_{-\infty}^{\infty}\int_{-\infty}^{\infty} (W_\psi f)(a,b)\overline{(W_\psi g)(a,b)}\frac{dbda}{a^2} = C_\psi (f,g). \qquad \ldots (55)$$

Proof. By Parseval's relation for the Fourier transforms, we have

$$\begin{aligned}(W_\psi f)(a,b) &= \int_{-\infty}^{\infty} f(t)|a|^{-\frac{1}{2}}\overline{\psi\left(\frac{t-b}{a}\right)}dt \\ &= (f, \psi_{a,b}) \\ &= (\hat{f}, \hat{\psi}_{a,b}) \\ &= \int_{-\infty}^{\infty} \hat{f}(x)|a|^{\frac{1}{2}} e^{ibx}\overline{\hat{\psi}(ax)}dx \\ &= (2\pi)^{1/2}\, \mathcal{F}\left\{|a|^{\frac{1}{2}}\hat{f}(x)\overline{\hat{\psi}(ax)}\right\}(-b)\end{aligned}$$

and

$$\begin{aligned}\overline{(W_\psi g)(a,b)} &= \int_{-\infty}^{\infty}\overline{g(t)}|a|^{-\frac{1}{2}}\psi\left(\frac{t-b}{a}\right)dt \\ &= \int_{-\infty}^{\infty}\overline{\hat{g}(y)}|a|^{\frac{1}{2}} e^{-iby}\hat{\psi}(ay)dy \\ &= (2\pi)^{1/2}\,\mathcal{F}\left\{|a|^{\frac{1}{2}}\hat{g}(x)\overline{\hat{\psi}(ax)}\right\}(-b).\end{aligned}$$

Then

$$\begin{aligned}&\int_{-\infty}^{\infty}\int_{-\infty}^{\infty}(W_\psi f)(a,b)\overline{(W_\psi g)(a,b)}\frac{dbda}{a^2} \\ &= 2\pi\int_{-\infty}^{\infty}\int_{-\infty}^{\infty}\mathcal{F}\left\{\hat{f}(x)\overline{\hat{\psi}(ax)}\right\}(b)\overline{\mathcal{F}\left\{\hat{g}(x)\hat{\psi}(ax)\right\}}(-b)\,db\,\frac{da}{a} \\ &= 2\pi\int_{-\infty}^{\infty}\int_{-\infty}^{\infty}\hat{f}(x)\overline{\hat{g}(x)}|\hat{\psi}(ax)|^2\,dx\,\frac{da}{a} \\ &= 2\pi\int_{-\infty}^{\infty}|\hat{\psi}(ax)|^2\frac{da}{a}\int_{-\infty}^{\infty}\hat{f}(x)\overline{\hat{g}(x)}dx \\ &= 2\pi\int_{-\infty}^{\infty}\frac{|\hat{\psi}(\omega)|^2}{|\omega|}d\omega\,(\hat{f},\hat{g}) \\ &= C_\psi(f,g),\end{aligned}$$

where Parseval's relation for the Fourier transform is used to justify the second and the fifth equality, and Fubini's theorem to justify the fourth one.

Theorem 3.4. (*Inversion Formula*). If $f \in L^2(R)$, then

$$f(t) = \frac{1}{C_\psi}\int_{-\infty}^{\infty}\int_{-\infty}^{\infty}(W_\psi f)(a,b)\psi_{a,b}(t)\frac{dbda}{a^2}, \qquad \ldots (56)$$

where the equality holds almost everywhere.

Proof. For any $g \in L^2(R)$, we have

$$\begin{aligned}C_\psi\langle f, g\rangle &= \langle W_\psi f, W_\psi g\rangle \\ &= \int_{-\infty}^{\infty}\int_{-\infty}^{\infty}(W_\psi f)(a,b)\overline{(W_\psi g)(a,b)}\frac{dbda}{a^2} \\ &= \int_{-\infty}^{\infty}\int_{-\infty}^{\infty}(W_\psi f)(a,b)\overline{\int_{-\infty}^{\infty}g(t)\overline{\psi_{a,b}(t)}dt}\cdot\frac{dbda}{a^2} \\ &= \int_{-\infty}^{\infty}\int_{-\infty}^{\infty}\int_{-\infty}^{\infty}(W_\psi f)(a,b)\psi_{a,b}(t)\cdot\frac{dbda}{a^2}\overline{g(t)}\,dt\end{aligned}$$

$$= \left(\int_{-\infty}^{\infty} \int_{-\infty}^{\infty} (W_\psi f)(a, b) \psi_{a,b} \frac{dbda}{a^2}, g \right).$$

Since g is an arbitrary element of $L^2(R)$, the inversion formula eq. (56) follows:

4 The Discrete Wavelet Transforms

It has been stated in the last section that the continuous wavelet transform eq. (38) is a two parameter representation of a function. In many applications, especially in signal processing, data are represented by a finite number of values, so it is important and often useful to consider discrete versions of the continuous wavelet transform eq. (38). From a mathematical point of view, a continuous representation of a function of two continuous parameters a, b in eq. (38) can be converted into a discrete one by assuming that a and b take only integral values. It turns out that it is better to discretize it in a different way. First, we fix two positive constants a_0 and b_0 and define

$$\psi_{m,n}(x) = a_0^{m/2} \psi\left(a_0^m x - n b_0\right), \quad \ldots (57)$$

where both m and $n \in Z$. Then for $f \in L^2(R)$, we calculate the discrete wavelet coefficients $(f, \psi_{m,n})$. The fundamental question is whether it is possible to determine f completely by its wavelet coefficients (discrete wavelet transform). The answer to this question is positive if the wavelets form a complete system in $L^2(R)$. The problem is whether there exists another function $g \in L^2(R)$ such that

$$(f, \psi_{m,n}) = (g, \psi_{m,n}) \text{ for all } m, n \in Z$$

implies that $f = g$.

In practice we expect much more than that: we want $(f, \psi_{m,n})$ and $(g, \psi_{m,n})$ to be "close" if f and g are "close". This will be guaranteed if there exists a $B>0$, independent of f, such that

$$\sum_{m,n=-\infty}^{\infty} \left| f, \tilde{\psi}_{m,n} \right|^2 \le B \|f\|^2. \quad \ldots (58)$$

Similarly, we want f and g to be "close" if $(f, \psi_{m,n})$ and $(g, \psi_{m,n})$ are "close". This is important because we want to be sure that when we neglect some small terms in the representation of f in terms of $(f, \psi_{m,n})$, then the reconstructed function will not differ much from f. The representation will have this property if there exists an $A>0$, independent of f, such that

$$A\|f\|^2 \le \sum_{m,n=-\infty}^{\infty} |(f, \psi_{m,n})|^2. \quad \ldots (59)$$

These two requirements are best studied in terms of the so-called frames.

Definition 4.1 (*Frames*). A sequence $\{\phi_1, \phi_2, \ldots\}$ in a Hilbert space H is called a *frame* if there exist A, $B>0$ such that

$$A\|f\|^2 \le \sum_{n=1}^{\infty} |(f, \phi_n)|^2 \le B\|f\|^2 \quad \ldots (60)$$

for all $f \in H$. The constants A and B are called *frame bounds*. If $A=B$, then the frame is called *tight*.

If $\{\phi_n\}$ is an orthonormal basis, then it is a tight frame since $\sum_{n=1}^{\infty} |(f, \phi_n)|^2 = \|f\|^2$ for all $f \in H$. The vectors $(1, 0)$, $\left(-\frac{1}{2}, \frac{\sqrt{3}}{2}\right), \left(-\frac{1}{2}, -\frac{\sqrt{3}}{2}\right)$ form a tight frame in C^2 which is not a basis.

As pointed out above, we want the family of functions $\psi_{m,n}$ to form a frame in $L^2(R)$. (Obviously, the double indexing of the functions is irrelevant). The following theorem gives fairly general, sufficient conditions for $(\psi_{m,n})$ to constitute a frame in $L^2(R)$.

Theorem 4.1 If ψ and a_0 are such that

(i) $$\inf_{1 \le |\omega| \le a_0} \sum_{m=-\infty}^{\infty} \left| \hat{\psi}\left(a_0^m \omega\right) \right|^2 > 0,$$

(ii) $$\sup_{1 \le |\omega| \le a_0} \sum_{m=-\infty}^{\infty} \left| \hat{\psi}\left(a_0^m \omega\right) \right|^2 > 0,$$

and

(iii) $$\sup_{\omega \in R} \sum_{m=-\infty}^{\infty} \left| \hat{\psi}\left(a_0^m \omega\right) \right| \left| \hat{\psi}\left(a_0^m \omega + x\right) \right| \le C\left(1 + |x|\right)^{-(1+\varepsilon)}$$

for some $\varepsilon > 0$ and some constant C, then there exists $\tilde{b}$ such that $\psi_{m,n}$ form a frame in $L^2(R)$ for any $b_0 \in (0, \tilde{b})$.

Since the proof is long and depends on the general Parseval formula for the Fourier transform, we refer to Debnath and Mikusinski[37].

The major problem of this section is reconstruction of f from $(f, \psi_{m,n})$ and representation of f in terms of $\psi_{m,n}$. For a complete orthonormal system $\{\phi_n\}$ both questions are answered by the equality

$$f = \sum_{n=1}^{\infty} (f, \phi_{m,n})\phi_n . \qquad \ldots (61)$$

However, since we do not have orthogonality, the problem is more complete for frames.

Definition 4.2 (*Frame Operator*). Let $\{\phi_1, \phi_2, \ldots\}$ be a frame in a Hilbert space H. The operator F from H into l^2 defined by

$$F\{f\} = \{(f, \phi_n)\}$$

is called a *frame operator.*

Lemma 4.1 Let F be a frame operator. Then F is a linear, invertible, and bounded operator. Its inverse F^{-1} is also a bounded operator.

The proof is easy and left as an exercise.

Consider the adjoint operator F^* of a frame operator F associated with frame $\{\phi_n\}$. For any $\{c_n\} \in l^2$, we have

$$(F^*(c_n), f) = ((c_n), Ff) = \sum_{n=1}^{\infty} c_n (\phi_n, f) = \left(\sum_{n=1}^{\infty} c_n \phi_n, f \right).$$

Thus the adjoint operator of a frame operator has the form

$$F^*(c_n) = \sum_{n=1}^{\infty} c_n \phi_n . \qquad \ldots (62)$$

Note also that since

$$\sum_{n=1}^{\infty} |(f, \phi_n)|^2 = \|Ff\|^2 = (F^* Ff, f),$$

the condition of eq. (60) can be expressed as

$$AI \le F^* F \le BI,$$

where the inequality $\le$ is to be understood in the sense defined in Section 4.6 (see Debnath and Mikusinski[37]).

Theorem 4.2 Let $\{\phi_1, \phi_2, \ldots\}$ be a frame bounds A and B and let F be the associated frame operator. Define

$$\tilde{\phi}_n = (F^* F)^{-1} \phi_n .$$

Then $\{\tilde{\phi}_n\}$ is a frame with frame bounds $\frac{1}{B}$ and $\frac{1}{A}$.

Proof. By Corollary 4.5.1 stated by Debnath and Mikusinski[37], we have $(F^* F)^{-1} = \left((F^* F)^{-1}\right)^*$. Consequently

$$\left(f, \tilde{\phi}_n\right) = \left(f, (F^* F)^{-1} \phi_n\right) = \left((F^* F)^{-1} f, \phi_n\right)$$

and then

$$\sum_{n=1}^{\infty} \left| \left(f, \{\tilde{\phi}_n\}\right) \right|^2 = \sum_{n=1}^{\infty} \left| \left((F^* F)^{-1} f, \phi_n\right) \right|^2$$

$$= \left\| F (F^* F)^{-1} f \right\|^2$$

$$= \left(F(F^* F)^{-1} f, F (F^* F)^{-1} f \right)$$

$$= \left((F^* F)^{-1} f, f \right).$$

Now, since $AI \le F^* F \le BI$, Theorem 4.6.5 proved by Debnath and Mikusinski[37] implies

$$\frac{1}{B} I \le (F^* F)^{-1} \le \frac{1}{A} I,$$

which gives

$$\frac{1}{B} \|f\|^2 \le \sum_{n=1}^{\infty} \left| \left(f, \{\tilde{\phi}_n\}\right) \right|^2 \le \frac{1}{A} \|f\|^2 .$$

This proves the theorem. The sequence $(\tilde{\phi}_n)$ is called the *dual frame.*

Lemma 4.2 Let F be the frame operator associated with the frame $\{\phi_1, \phi_2 \ldots\}$ and let $\tilde{F}$ be the frame operator associated with the dual frame $\{\tilde{\phi}_1, \tilde{\phi}_2, \ldots\}$. Then

$$\tilde{F}^* F = I = F^* \tilde{F} .$$

Proof. Since

$$F (F^* F)^{-1} f = \left\{ \left((F^* F)^{-1} f, \phi_n \right) \right\} = \left\{ \left(f, \tilde{\phi}_n \right) \right\} = \tilde{F} f,$$

we have

$$\tilde{F}^* F = \left(F (F^* F)^{-1} \right)^* F = (F^* F)^{-1} F^* F = I$$

and

$$F^* \tilde{F} = F^* F (F^* F)^{-1} = I.$$

Now we are ready to state and prove the main theorem which answers the question of reconstructibility of f from $\{(f, \phi_n)\}$.

Theorem 4.3 Let $\{\phi_1, \phi_2, \ldots\}$ constitute a frame in a Hilbert space H and let $\{\tilde{\phi}_1, \tilde{\phi}_2, \cdots\}$ be the dual frame. Then

$$f = \sum_{n=1}^{\infty} (f, \phi_n) \tilde{\phi}_n$$

and

$$f=\sum_{n=1}^{\infty}(f,\tilde{\phi}_n)\phi_n$$

for any $f\in H$.

Proof. Let f be the frame operator associated with $\{\tilde{\phi}_n\}$ and let $\tilde{F}$ be the frame operator associated with the dual frame $\{\phi_n\}$. Since $I=\tilde{F}^*F$, for any $f\in H$, we have

$$f=\tilde{F}^*Ff=\tilde{F}^*\{(f,\phi_n)\}=\sum_{n=1}^{\infty}(f,\phi_n)\tilde{\phi}_n,$$

by eq. (62). The proof of the other equality is similar.

5 Multiresolution Analysis and Construction of Wavelets

Some difficulties in dealing with frames arise from lack of orthogonality. If we have the orthogonality, that is $(\psi_{k,l}, \psi_{m,n})=0$ whenever $(k, l)\neq(m, n)$, then the reconstruction of f from $(f, \psi_{m,n})$ is much simpler and f assumes the form $f=\sum_{m,n=-\infty}^{\infty}(f,\psi_{m,n})\psi_{m,n}$.

The Haar wavelets, described in Theorem 3.1, clearly form an orthonormal system. In this section we describe a general method of constructing orthonormal bases of wavelets based on the so-called multiresolution analysis. In this construction we take $a_0=2$ and $b_0=1$. Consequently,

$$\phi_{m,n}(x)=2^{m/2}\phi(2^m x-n). \qquad \ldots(63)$$

The fundamental idea of multiresolution analysis is to represent a function as a limit of successive approximations, each of which is a "smoother" version of the original function. These approximations correspond to different resolutions. Multiresolution analysis is a formal approach to constructing orthogonal wavelet bases using a definite set of rules and procedures. In applications, it is an effective mathematical framework for hierarchical decomposition of a signal or an image into components of different scales. The spaces V_n correspond to those different scales.

Definition 5.1 (*Multiresolution Analysis*). A multiresolution analysis (MRA) consists of a sequence $\{V_n\}$, $n\in Z$ of closed subspaces of functions $f\in L^2(R)$ defined on R such that the following conditions are satisfied:

(a) $V_n\subset V_{n+1}$ for all $n\in Z$,

(b) $\bigcup_{n=-\infty}^{\infty}V_n$ is dense in $L^2(R)$ and $\bigcap_{n=-\infty}^{\infty}V_n=\{0\}$,

(c) $f\in V_n$ if and only if $f(2x)\in V_{n+1}$ for all $n\in Z$,

(d) there exists a function $\phi\in V_0$ such that $\{\phi_{0,k}=\phi(x-k): k\in Z\}$ is an orthonormal basis for V_0.

The function ϕ is called a *scaling function.*

It easily follows from Definition 5.1 that

(i) V_0 is invariant under translation by an integer, that is, $T_kV_0=V_0$,

(ii) $f\in V_n$ if and only if $f(2^nx)\in V_0$ for all $n\in Z$, that is, all the spaces are scaled versions of the central space V_0,

(iii) $V_n=D_{2^{-n}}T_kV_0=\{f(2^nx-k): f\in V_0\}$,

(iv) for every $m\in Z$, $\{\phi_{m,n}(x)=2^{\frac{m}{2}}\phi(2^mx-n)\}_{n=-\infty}^{n=\infty}$ is an orthonormal basis for V_m.

Example 5.1 Suppose V_m is the space of all functions in $L^2(R)$ which are constant on intervals $[2^{-m}n, 2^{-m}(n+1)]$, $n\in Z$. Then $\{V_m: m\in Z\}$ is an MRA and the scaling function may be chosen as the characteristic function $\phi=\chi_{[-1\,0]}$. Clearly, $\phi(t)$, $\phi(t-n)$ are orthornomal since their product is.

Suppose $\phi_{m,n}(x)=2^{\frac{m}{2}}\phi(2^mx-n)$. Since $\phi_{0,n}(x)=\phi(x-n)\in V_0$ for all $n\in Z$ due to (d) in Definition 5.1. Further, if $m\in Z$, condition (c) implies that $\{\phi_{m,n}: n\in Z\}$ is an orthonormal basis for V_m.

The spaces in a multiresolution analysis form a ladder

$$\cdots V_{-m}\subset\cdots\subset V_{-2}\subset V_{-1}\subset V_0\subset V_1\subset V_2\subset\cdots\subset V_m\cdots.$$

If any of the spaces V_n is given, then, by (ii), any other spaces V_m is known because

$$V_m=\{f(2^{n-m}x): f\in V_n\}$$

In most cases concerning multiresolution analysis, it is sufficient to deal with the central space V_0. Note that a multiresolution analysis is completely determined by the scaling function ϕ. In fact, for a given ϕ, we first define

$$V_0 = \left\{ \sum_{n=-\infty}^{\infty} c_n \phi_{0,n} : \{c_n\} \in l^2(Z) \right\}.$$

The remaining spaces V_n are then determined by V_0 as discussed above. Of course, it is not obvious that any choice of ϕ will produce a multiresolution analysis. The first problem is the orthonormality of translates of ϕ. The following theorem can be helpful for this problem.

Theorem 5.1 For any $\phi \in L^2(R)$ the following two conditions are equivalent

(a) the system $\{\phi_{0,k} : k \in Z\}$ is orthonormal

(b) $$\sum_{m=-\infty}^{\infty} \left| \hat{\phi}(\omega + 2m\pi) \right|^2 = \frac{1}{2\pi}$$ almost everywhere

Proof. Since

$$\hat{\phi}_{0,k}(\omega) = e^{-ik\omega} \hat{\phi}(\omega)$$

we have

$$\begin{aligned}
(\phi_{0,k}, \phi_{0,l}) &= (\phi_{0,0}, \phi_{0,l-k}) = (\hat{\phi}_{0,0}, \hat{\phi}_{0,l-k}) \\
&= \int_{-\infty}^{\infty} e^{-i(l-k)\omega} \left| \hat{\phi}(\omega) \right|^2 d\omega \\
&= \sum_{m=-\infty}^{\infty} \int_{2m\pi}^{2(m+1)\pi} e^{-i(l-k)\omega} \left| \hat{\phi}(\omega) \right|^2 d\omega \\
&= \int_0^{2\pi} e^{-i(l-k)\omega} \sum_{m=-\infty}^{\infty} |\hat{\phi}(\omega + 2m\pi)|^2 \, d\omega.
\end{aligned}$$

Thus $(\phi_{0,k}, \phi_{0,l}) = \delta_{k,l}$ if and only if $$\sum_{m=-\infty}^{\infty} \left| \hat{\phi}(\omega + 2m\pi) \right|^2 = \frac{1}{2\pi}$$ almost everywhere.

Once the scaling function ϕ is known, we may use it to construct the mother wavelet, ψ such that $\{\psi(x-n)\}$ is an orthonormal basis of the space W_0 given by the orthogonal complement of V_0 in V_1. Then $V_1 = V_0 \oplus W_0$ where $\oplus$ is the direct sum. If such a ψ can be found, then

$$\psi_{m,n}(x) = 2^{m/2} \psi\left(2^{m/2} x - n\right), n \in Z, \quad \ldots (64)$$

is an orthonormal basis of W_m. This is the dilated space of W_0, and will be the orthogonal complement of V_m in V_{m+1}. Hence we have

$$V_{m+1} = V_m \oplus W_m \text{ and } W_m \perp W_n \text{ for } m \neq n.$$

Further,

$$\begin{aligned}
V_{m+1} &= V_m \oplus W_m \\
&= V_{m-1} \oplus W_{m-1} \oplus W_m \\
&= V_{m-2} \oplus W_{m-2} \oplus W_{m-1} \oplus W_m \\
&= \cdots \\
&= V_0 \oplus W_0 \oplus W_1 \oplus \cdots \oplus W_{m-1} \oplus W_m. \quad \ldots (65)
\end{aligned}$$

Since $\bigcup_{m=-\infty}^{\infty} V_m$ is dense in $L^2(R)$, we may take the limit as $m \to \infty$ to obtain

$$V_0 \oplus \left(\bigoplus_{m=0}^{\infty} W_m \right) = L^2(R).$$

We may also go in the other direction to write

$$V_0 = W_{-1} \oplus W_{-1} = V_{-2} \oplus W_{-2} \oplus W_{-1} = V_{-k} \oplus W_{-k} \oplus \cdots \oplus W_{-1}.$$

Since $\bigcap_{m=-\infty}^{\infty} V_m = \{0\}$, it follows that $V_{-k} \to \{0\}$ as $k \to \infty$, we obtain

$$\bigoplus_{m=-\infty}^{\infty} W_m = L^2(R). \quad \ldots (66)$$

This represents a decomposition of $L^2(R)$ into mutually orthogonal subspaces. Moreover, for all $m \in Z$,

$f \in W_m$ if and only if $f\left(2^m x\right) \in W_0$.

This is a very desirable property because if $\{\theta_k : k \in Z\}$ is an orthonormal basis for W_0, then the scaled version $\{\theta(2^n x) : k \in Z\}$ is an orthonormal basis for W_n, *for* every $n \in Z$. This fact, together with eq. (63), implies that the union of all these bases, that is $\{\theta_k(2^n, \cdot) : k, n \in Z\}$ is an orthonormal basis for $L^2(R)$. Note that the spaces V_n do not have this property. This is the reason for defining the spaces W_n.

The property just described reduces the problem of finding an orthonormal basis for W_0. We want to go one step further: we want to find a single function ψ such that the translates $\{\psi_{0,n} : n \in Z\}$ constitute an orthonormal basis in W_0. If we can find a function like that, then the system $\{\psi_{m,n} : m, n \in Z\}$, will be an orthonormal basis for $L^2(R)$. It will be an orthonormal basis of wavelets. It turns out that such a ψ exists for every multiresolution analysis. The proof of this fact not only guarantees existence of such a function, but actually gives a method of constructing it. The function ψ is often called the *mother wavelet.*

We start the construction by introducing an auxiliary function M_0 which plays an important

role in the analysis. Since $\phi \in V_1$ and $(\phi_{1,n})$ is an orthonormal basis for V_1, we can express ϕ in the form

$$\phi = \sum_{n=-\infty}^{\infty} h_n \phi_{1,n} \text{ or } \phi(x) = \sqrt{2} \sum_{n=-\infty}^{\infty} h_n \phi(2x-n), \quad \ldots (67)$$

where

$$h_n^* = (\phi, \phi_{1,n}) \text{ and } \sum_{n=-\infty}^{\infty} |h_n|^2 = 1.$$

Applying the Fourier transform to eq. (66) gives

$$\hat{\phi}(s) = \frac{1}{\sqrt{2}} \sum_{n=-\infty}^{\infty} h_n e^{-ins/2} \hat{\phi}(s/2). \quad \ldots (68)$$

If we define

$$M_0(s) = \frac{1}{\sqrt{2}} \sum_{n=-\infty}^{\infty} h_n e^{-ins} \quad \ldots (69)$$

then eq. (68) can be written as

$$\hat{\phi}(s) = M_0(s/2) \hat{\phi}(s/2). \quad \ldots (70)$$

By Theorem 5.1, we have

$$\sum_{k=-\infty}^{\infty} \left| \hat{\phi}(s+2k\pi) \right|^2 = \frac{1}{2\pi} \quad \ldots (71)$$

which, together with eq. (70), gives

$$\sum_{k=-\infty}^{\infty} |M_0(s+k\pi)|^2 \left| \hat{\phi}(s+k\pi) \right|^2 = \frac{1}{2\pi} \text{ a.e.} \quad \ldots (72)$$

By splitting the sum into even and odd k and then using 2π-periodicity of M_0, we obtain

$$\sum_{k=-\infty}^{\infty} |M_0(s+k\pi)|^2 \left| \hat{\phi}(s+k\pi) \right|^2 = \sum_{k=-\infty}^{\infty} |M_0(s+2k\pi)|^2 \left| \hat{\phi}(s+2k\pi) \right|^2 + \sum_{k=-\infty}^{\infty} |M_0(s+(2k+1)\pi)|^2 \left| \hat{\phi}(s+(2k+1)\pi) \right|^2$$

$$= \sum_{k=-\infty}^{\infty} |M_0(s)|^2 \left| \hat{\phi}(s+2k\pi) \right|^2 + \sum_{k=-\infty}^{\infty} |M_0(s+\pi)|^2 \left| \hat{\phi}(s+\pi+2k\pi) \right|^2$$

$$= \left(|M_0(s)|^2 + |M_0(s+\pi)|^2 \right) \frac{1}{2\pi}.$$

by eq. (71) used in its original form and with s replaced by $s+\pi$. Now eq. (71) implies

$$|M_0(s)|^2 + |M_0(s+\pi)|^2 = 1 \text{ a.e.} \quad \ldots (73)$$

Now we state a technical lemma.

Lemma 5.1 For every $f \in W_0$ there exists a 2π-periodic function ν such that

$$\hat{f}(s) = \nu(s) e^{is/2} \overline{M_0(s/2+\pi)} \hat{\phi}(s/2). \quad \ldots (74)$$

Note that $e^{is/2} \overline{M_0(s/2+\pi)} \hat{\phi}(s/2)$ in eq. (73) is independent of f.

Now we return to our main problem. Suppose that we found a function ψ such that $\{\psi_{0,n} : n \in Z\}$ is a basis for W_0. Then every function f from W_0 has a representation

$$f = \sum_{n=-\infty}^{\infty} \gamma_n \psi_{0,n} \quad \ldots (75)$$

where $\sum_{n=-\infty}^{\infty} |\gamma_n|^2 < \infty$. We apply the Fourier transform to eq. (75) to obtain

$$\hat{f}(s) = \left(\sum_{n=-\infty}^{\infty} \gamma_n e^{-ns} \right) \hat{\psi}(s) \quad \ldots (76)$$

The function $\gamma(s) = \sum_{n=-\infty}^{\infty} \gamma_n e^{-ns}$ is a 2π-periodic function, square integrable on $[0, 2\pi]$. When this is compared with eq. (74), then we see that we should take

$$\hat{\psi}(s) = e^{is/2} \overline{M_0(s/2+\pi)} \hat{\phi}(s/2).$$

Since

$$\hat{\psi}(s) = e^{is/2} \overline{M_0(s/2+\pi)} \hat{\phi}(s/2)$$

$$= e^{is/2} \frac{1}{\sqrt{2}} \sum_{n=-\infty}^{\infty} h_n e^{in(s/2+\pi)} \hat{\phi}(s/2)$$

$$= \frac{1}{\sqrt{2}} \sum_{n=-\infty}^{\infty} h_n e^{in\pi} e^{i(n+1)(s/2)} \hat{\phi}(s/2),$$

we have

$$\psi(x) = \sqrt{2} \sum_{n=-\infty}^{\infty} (-1)^{n-1} h_{-n-1} \phi(2x-n).$$

This leads to the main theorem of this section:

Theorem 5.2 Let (V_n), $n \in Z$ be a multiresolution analysis with the scaling function ϕ. Then the function

$$\psi(x) = \sqrt{2} \sum_{n=-\infty}^{\infty} (-1)^{n-1} h_{-n-1} \phi(2x-n), \quad \ldots (77)$$

is a mother wavelet, that is, the system $\{\psi_{m,n}: m,n\in Z\}$, is an orthonormal basis for $L^2(R)$, where

$$h_n = \int_{-\infty}^{\infty} \phi(x)\overline{\phi(2x-n)}\,dx. \qquad \ldots(78)$$

Proof First we need to verify that $\{\psi_{0,n}: m,n\in Z\}$ is an orthonormal set. Indeed, we have

$$\int_{-\infty}^{\infty} \psi(x-k)\overline{\psi(x-l)}\,dx = \int_{-\infty}^{\infty} e^{-is(k-l)}\left|\hat{\psi}(s)\right|^2 ds$$
$$= \int_0^{2\pi} e^{-is(k-l)} \sum_{n=-\infty}^{\infty} \left|\psi(s+2n\pi)\right|^2 ds$$

and

$$\sum_{n=-\infty}^{\infty} \left|\hat{\psi}(s+2n\pi)\right|^2 = \sum_{n=-\infty}^{\infty} \left|M_0(s/2+(n+1)\pi)\right|^2 \left|\hat{\phi}(s/2+n\pi)\right|^2$$
$$= \sum_{n=-\infty}^{\infty} \left|M_0(s/2+(2n+1)\pi)\right|^2 \left|\hat{\phi}(s/2+2n\pi)\right|^2$$
$$+ \sum_{n=-\infty}^{\infty} \left|M_0(s/2+(2n+2)\pi)\right|^2 \left|\hat{\phi}(s/2+(2n+1)\pi)\right|^2$$
$$= \left|M_0(s/2+\pi)\right|^2 \sum_{n=-\infty}^{\infty} \left|\hat{\phi}(s/2+2n\pi)\right|^2$$
$$+ \left|M_0(s/2)\right|^2 \sum_{n=-\infty}^{\infty} \left|\hat{\phi}(s/2+(2n+1)\pi)\right|^2$$
$$= \left(\left|M_0(s/2+\pi)\right|^2 + \left|M_0(s/2)\right|^2\right)\frac{1}{2\pi}$$
$$= \frac{1}{2\pi}.$$

Thus

$$\int_{-\infty}^{\infty} \psi(x-k)\overline{\psi(x-l)}\,dx = \delta_{k,l},$$

which proves that $\{\psi_{m,n}: m,n\in Z\}$ is an orthonormal system. In view of Lemma 5.1 and the discussion preceeding the theorem, to prove that it is a basis, it suffices to show that the function v in eq. (74) is square integrable over $[0,2\pi]$. It can be shown that there exists a function λ such that $M_f(s)=\lambda(s)\overline{M_0(s+\pi)}$ a.e., where

$$M_f(s) = \frac{1}{\sqrt{2}} \sum_{n=-\infty}^{\infty} c_n \exp(-ins).$$

Since M_0 and M_f are 2π-periodic, so is λ. Moreover $\lambda(s)+\lambda(s+\pi)=0$ a.e. There exists a 2π-periodic function v defined by $\lambda(s)=\exp(is)v(2s)$. In fact,

$$\int_0^{\infty} |v(s)|^2 ds = 2\int_0^{\pi} |\lambda(s)|^2 ds$$
$$= 2\int_0^{\pi} |\lambda(s)|^2 \left(\left|M_0(s+\pi)\right|^2 + \left|M_0(s)\right|^2\right) ds$$
$$= 2\int_0^{2\pi} |\lambda(s)|^2 \left|M_0(s+\pi)\right|^2 ds$$
$$= 2\int_0^{2\pi} \left|M_f(s)\right|^2 ds$$
$$= 2\pi \sum_{n=-\infty}^{\infty} |c_n|^2, \text{ where } c_n = (f, \phi_{1,n})$$
$$= 2\pi \|f\|^2 < \infty.$$

Example 5.2 *(The Shannon System).* If

$$\hat{\phi} = \begin{cases} \frac{1}{\sqrt{2\pi}} & -\pi \le s < \pi \\ 0 & \text{otherwise} \end{cases},$$

then

$$\sum_{m=-\infty}^{\infty} \left|\hat{\phi}(s+2m\pi)\right|^2 = \frac{1}{2\pi} \text{ a.e.}$$

Since

$$\phi(x) = \frac{\sin \pi x}{\pi x},$$

the system

$$\phi_{0,k}(x) = \frac{\sin \pi(x+k)}{\pi(x+k)}, \; k \in Z,$$

is orthonormal. Now, as indicated in the general case, we define

$$V_0 = \left\{ \sum_{k=-\infty}^{\infty} c_k \frac{\sin \pi(x+k)}{\pi(x+k)} : \sum_{k=-\infty}^{\infty} |c_k|^2 < \infty \right\}$$

and, for other $n\in Z$,

$$V_n = \left\{ \sum_{k=-\infty}^{\infty} c_k \frac{2^{n/2} \sin \pi(2^n x+k)}{\pi(2^n x+k)} : \sum_{k=-\infty}^{\infty} |c_k|^2 < \infty \right\}.$$

We can check that all the conditions of Definition 5.1 are satisfied. Next, we have to find the coefficients h_n:

$$h_n = \int_{-\infty}^{\infty} \phi(x)\phi(2x-n)\,dx$$

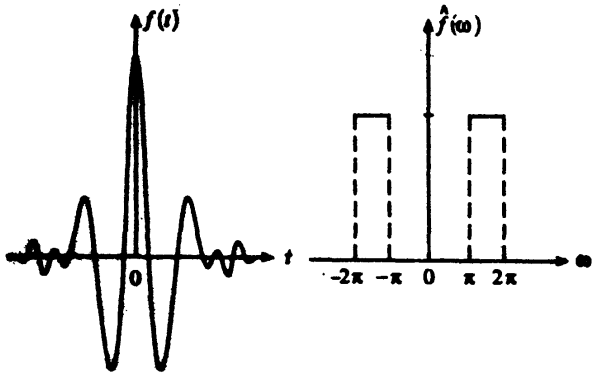

Fig. 6 The Shannon Wavelet and its Fourier Transform

$$= \int_{-\infty}^{\infty} \frac{\sin \pi x}{\pi x} \frac{\sin \pi (2x-n)}{\pi (2x-n)} dx$$

$$= \begin{cases} \frac{1}{2} & \text{if } n = 0 \\ \frac{1}{\pi n} \sin \frac{\pi n}{2} & \text{otherwise.} \end{cases}$$

Consequently,

$$\psi(x) = \sqrt{2} \sum_{n=-\infty}^{\infty} (-1)^{n-1} h_{-n-1} \phi(2x-n)$$

$$= \frac{1}{\sqrt{2}} \frac{\sin \pi (2x+1)}{\pi (2x+1)} + \sqrt{2} \sum_{n \neq -1} \frac{(-1)^{n-1}}{\pi (-n-1)} \sin \frac{\pi (-n-1)}{2} \frac{\sin \pi (2x-n)}{\pi (2x-n)}$$

$$= \frac{1}{\sqrt{2}} \frac{\sin \pi (2x+1)}{\pi (2x+1)} + \sqrt{2} \sum_{n \neq -1} \frac{(-1)^{n-1}}{\pi (n+1)} \cos\left(\frac{\pi n}{2}\right) \frac{\sin \pi (2x-n)}{\pi (2x-n)}$$

is a mother wavelet for which the system $\{\psi_{m,n} : m,n \in Z\}$ is an orthonormal basis in $L^2(R)$. It is known as the *Shannon system*. It has interesting applications in sampling theory (Fig.6).

6 Daubechies' Construction of Wavelets

For the wavelets to be useful analyzing functions, the mother wavelet must satisfy certain desirable properties. One such property is defined by the condition eq. (37) which guarantees the existence of the inversion formula for the continuous wavelet transform. If $\psi \in L^1(R)$, then its Fourier transform $\hat{\psi}(\omega)$ is continuous, and hence C_ψ can be finite only if $\hat{\psi}(0)=0$ which implies that ψ has zero average, that is

$$\int_{-\infty}^{\infty} \psi(t) dt = 0. \quad \ldots (79)$$

This means that a wavelet must be an oscillatory function with zero mean. Condition (37) also suggests that $|\hat{\psi}(\omega)|^2$ decays at least as $|\omega|^{-1}$. Therefore, the wavelet $\psi(t)$ must decay at least as $|t|^{-\varepsilon-1}$ for some $\varepsilon > 0$. In addition to condition (37), there are other desirable properties for a function to be a useful wavelet which are as follows :

(i) *Smoothness* : $\psi(t)$ should be *smooth*, that is, it is n times differentiable with continuous derivatives.

(ii) *Localization* : $\psi(t)$ should be well localized both in time and frequency domains. In other words, $\psi(t)$ and its derivatives must decay very rapidly. For frequency localization, $\hat{\psi}(\omega)$ must decay sufficiently rapidly as $|\omega| \to \infty$ and $\hat{\psi}(\omega)$ should be flat in the neighbourhood of ω=0. This property of flatness at ω=0 is associated with the number of vanishing moments of $\psi(t)$. The kth moment of $\psi(t)$ is defined by

$$m_k = \int_{-\infty}^{\infty} t^k \psi(t) dk. \quad \ldots (80)$$

For a wavelet to have n vanishing moment if eq. (80) holds for k=0, 1, . . . , n. Or, equivalently,

$$\left[\frac{d^k \hat{\psi}(\omega)}{d\omega^k} \right]_{\omega=0} = 0 \text{ for } k = 0, 1, \ldots, n. \quad \ldots (81)$$

Wavelets with a larger number of vanishing moments result in more flatness when the frequency ω is small.

Thus the properties (i) and (ii) combined with condition (37) reveal that

(a) wavelets are band-pass filters, that is, the frequency response decays very rapidly as $|\omega| \to \infty$, and is zero in the vicinity of ω=0.

(b) $\omega(t)$ is the impulse response of the filter, and it also decays very rapidly as time t increases. Moreover, it is an oscillating function with zero-mean. It has already been stated that ψ must be an absolutely square integrable function, that is, $\psi \in L^2(R)$.

In general, we may not have an explicit representation of $\psi_{m,n}(x)$. As suggested by Daubechies[17] and Strang[38], the construction of

wavelets starts with the solution of a *dilation equation* for a scaling function in the form

$$\phi(x)=\sum c_k\,\phi(2x-k). \qquad \ldots(82)$$

The function ϕ has compact support if and only if a finite number of coefficients c_k are non-zero. Translations of the scaling function, $\{\phi(x-k)\}_{k\in Z}$ form a Riesz or unconditional basis of a subspace $V_n \subset L^2(R)$. Furthermore, we can obtain a Riesz basis $\{\phi_{n,k}(x)\}$ for the subspace $V_n \subset L^2(R)$ by translating ϕ by a factor or k and dilating by a factor of 2^n so that

$$\phi_{n,k}=2^{n/2}\phi\left(2^n x-k\right) \qquad \ldots(83)$$

corresponding to resolution level n.

If translations of the scaling function ϕ at some resolution level n satisfy the condition

$$\int_{-\infty}^{\infty}\varphi_{n,k}(x)\phi_{n,l}(x)dx=\delta_{kl}, \qquad \ldots(84)$$

where $n, k, l \in Z$, then $\phi(x)$ is orthonormal. In this case, the best approximation of a function $f\in L^2(R)$ is given by the orthogonal projection of f on $V_n \subset L^2(R)$ as follows :

$$A_n f(x)=\sum_k a_{n,k}\,\phi_{n,k}(x), \qquad \ldots(85)$$

where the function $A_n f \in V_n$ at the given resolution level n and $a_{n,k}$ is given by the inner product

$$a_{n,k}=\left(f,\phi_{n,k}\right)=\int_{-\infty}^{\infty} f(x)\phi_{n,k}(x)dx. \qquad \ldots(86)$$

The operator A_n is a linear orthogonal projection operator[11,12] resulting in the best approximation of $f(x)$ in V_n. Then the mother wavelet ψ is given in terms of the scaling function ϕ as

$$\psi(x)=\sum_k (-1)^k c_{1-k}\,\phi(2x-k). \qquad \ldots(87)$$

The construction of the Daubechies wavelets begins with the finding of a sequence c_k for a finite number of non-zero terms (k=0, 1, ..., $2N$–1) involved in eq. (81) where N represents an index of the wavelet functions. Obviously, this index determines the number of non-zero coefficients c_k, the support and the regularity of the wavelet functions. N=1 corresponds to the Haar wavelet given in Example 3.1. Daubechies[17] determined the numerical values of the reconstruction and decomposition sequences for different values (not unique) of the index N. For low order bases, the reconstruction sequence has the explicit representation. For example, the non-zero coefficients c_k for the scaling function ϕ are as follows :

$$N=2:\left\{\begin{array}{ll} c_0=\frac{1}{4}\left(1+\sqrt{3}\right), & c_1=\frac{1}{4}\left(3+\sqrt{3}\right) \\ c_2=\frac{1}{4}\left(3-\sqrt{3}\right), & c_2=\frac{1}{4}\left(1-\sqrt{3}\right) \end{array}\right\}$$

$$N=3: c_0=\frac{1}{16}\left(1+\sqrt{10}+\sqrt{5+2\sqrt{10}}\right),$$

$$c_1=\frac{1}{16}\left(5+\sqrt{10}+3\sqrt{5+2\sqrt{10}}\right),$$

$$c_2=\frac{1}{16}\left(10-2\sqrt{10}+2\sqrt{5+2\sqrt{10}}\right),$$

$$c_3=\frac{1}{16}\left(10-2\sqrt{10}-2\sqrt{5+2\sqrt{10}}\right),$$

$$c_4=\frac{1}{16}\left(5+\sqrt{10}-3\sqrt{5+2\sqrt{10}}\right),$$

$$c_5=\frac{1}{16}\left(1+\sqrt{10}-\sqrt{5+2\sqrt{10}}\right).$$

Since Daubechies' wavelets are orthogonal, the non-zero coefficients for the wavelet function ψ are

$$d_k=(-1)^k c_{1-k}, \quad k=2-2N,\ldots,1.$$

These coefficients c_k and d_k have only a finite number of non-zero terms. The decomposition sequences e_k and f_k are given by

$$e_k=c_{-k}, \quad k=0,\ldots,2N-1,$$
$$f_k=d_{-k}, \quad k=2-2N,\ldots,1.$$

The support for the scaling and wavelet functions are given by

$$\text{supp}\,(\phi_{n,k})=[2^{-n}k, 2^{-n}(k+2N-1)],$$

$$\text{supp}\,(\psi_{n,k})=[2^{-n}(k+1-N), 2^{-n}(k+N)].$$

Both $\phi_{n,k}(x)$, $\psi_{n,k}(x)\in C^{\lambda_N}$, that is, they belong to the space of Hölder continuous functions C^{λ_N} with index λ_N, which satisfy the condition

$$\left|f^{(k)}(x)-f^{(k)}(x+h)\right|\le K|h|^{\alpha}, \qquad \ldots(88)$$

where $k=[\lambda_N]$; $0\le\alpha=\lambda_N-k<1$ and K is a positive constant. Note that the wavelet order N determines the value of the order λ_N. The differentiability of the wavelets increases with the order N. When

N=2, the Daubechies wavelet is everywhere continuous, left-differentiable at dyadic points $x=k\cdot 2^{-n}$, and nowhere right differentiable at these points. Daubechies and Legarias[39,40] computed the continuity of the bases as, $\lambda_2\approx 0.55$, $\lambda_3\approx 1.088$, $\lambda_4\approx 1.617$. For larger N, $\lambda_N\approx(0.3485)N$. The Daubechies wavelet bases also have zero moments of order N, that is,

$$m_k = \int_{-\infty}^{\infty} x^k \psi(x)dx = 0 \quad \text{for } k = 0,1,\ldots, N-1.$$

This leads to the fact that the scaling bases can be represented by polynomials of degree (N–1) exactly. The Daubechies scaling and wavelet functions of order N=3 and N=4 are shown in Figs. 7 and 8 respectively.

Example 6.1 *(Battle-Lemarie Wavelets).* Battle[14] used linear B-splines to construct orthogonal wavelet bases with exponential decay. The wavelet obtained is a polynomial of degree n–2 and n vanishing moments. The scaling function is

$$\phi(t) = \begin{cases} 1-|t|, & 0 \le |t| < 1 \\ 0, & \text{otherwise} \end{cases},$$

and has compact support. Battle-Lemarie's scaling function and wavelet are shown in Figs 9(a) and (b). It is noted that this wavelet does not have compact support, but it decays rapidly.

7 The Weierstrass and Riemann Non-differentiable Functions

In 1872, Weierstrass introduced a famous everywhere continuous but nowhere differentiable function defined by

$$\sigma(t) = \sum_{n=0}^{\infty} \alpha^n \cos(\beta^n t), \; 0 < \beta < 1. \qquad \ldots (89)$$

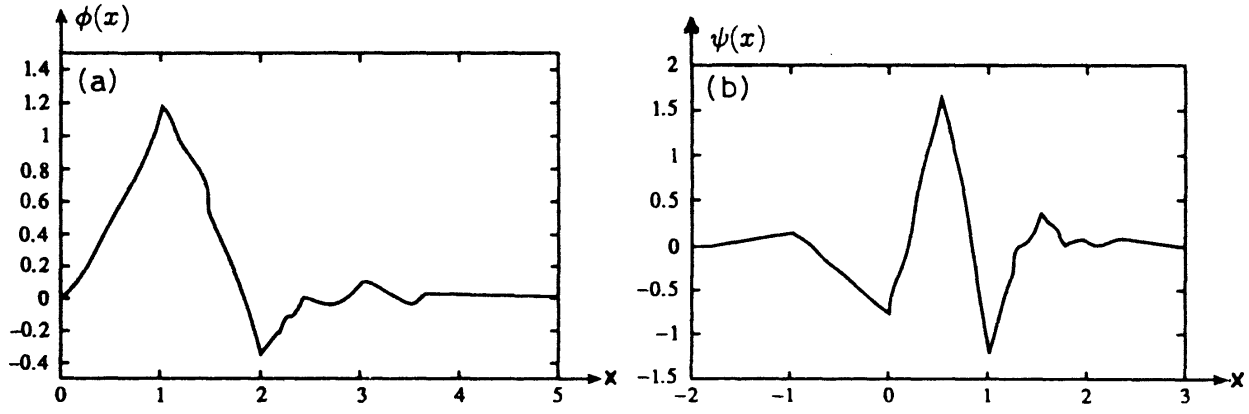

Fig. 7 For N=3, (a) scaling function, $\phi(x)$ and (b) wavelet function, $\psi(x)$.

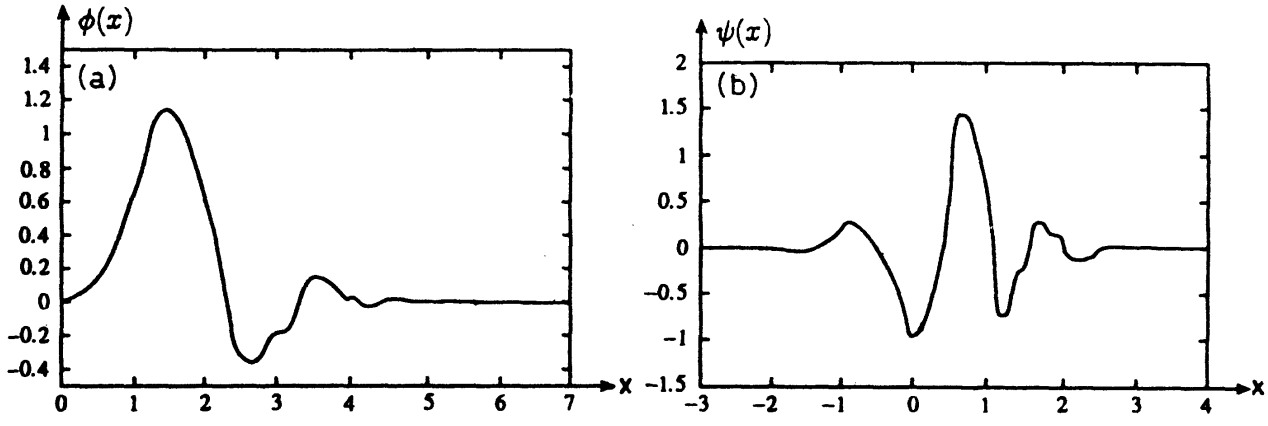

Fig. 8 For N=4, (a) scaling function, $\phi(x)$ and (b) wavelet functions, $\psi(x)$.

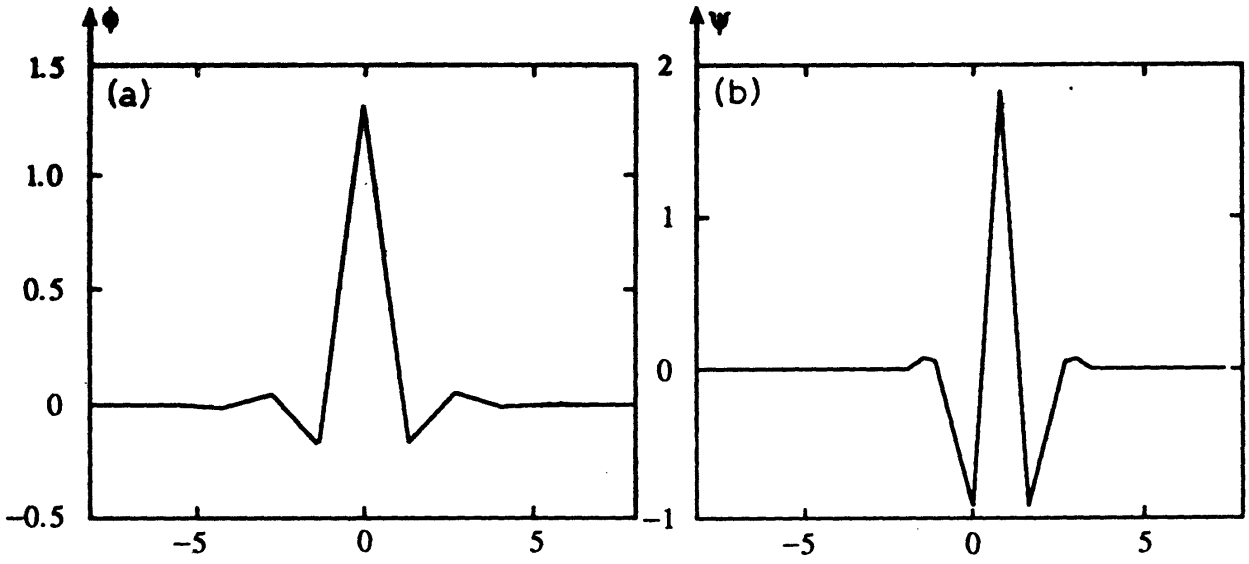

Fig. 9(a) Battle-Lemarie scaling function, (b) Battle-Lemarie wavelet.

He found that if α is an odd integer and $\alpha\beta$ is sufficiently large, then $\sigma(t)$ is nowhere differentiable. Later, Hardy studied the problem and showed that $\alpha\beta \geq 1$ is sufficient.

In recent years, the wavelet transform analysis is successfully used to simplify the proof of non-differentiability of both the Weierstrass and Riemann functions. A direct computation in Fourier transform space leads to the result

$$W_\psi |f|(a,b) = \sum_{n=1}^{\infty} \alpha^n \hat{\psi}(\alpha\beta^n) \exp(ib\beta^n), \quad \ldots (90)$$

where $f \in S_+(R)$ such that supp $\hat{\psi} \subset [1, \beta]$. It turns out that different frequencies decouple and then

$$|W_\psi [f](a,b)| = \sum_{n=1}^{\infty} \alpha^n |\hat{\psi}(\alpha\beta^n)|. \quad \ldots (91)$$

If we choose $\alpha_m = \beta^{-m}$, the above function does not decay with $0(a)$, confirming that $\sigma(t)$ is non-differentiable. Even if $\alpha\beta=1$, it can be shown that σ is non-differentiable.

Another famous everywhere continuous but nowhere differentiable function is introduced by Riemann in the form

$$W(t) = \sum_{n=1}^{\infty} \frac{1}{n^2} \sin(\pi n^2 t). \quad \ldots (92)$$

In 1916, Hardy proved that this function is non-differentiable at any irrational point and also at certain specific rational points. Fifty-four years later, Gerver (1970) proved that W is differentiable at any rational point $t = \frac{p}{q}$ where p and q are odd integer.

In recent years, Holschneider[41] and Holschneider and Tchamitchian[42] have successfully utilized the wavelet transform to reinvestigate the function W by considering a family of functions W_β in the form

$$W_\beta(t) = \frac{2}{\pi^\beta} \sum_{n=1}^{\infty} n^{-2\beta} \exp(i\pi tn^2), \beta > \frac{1}{2}. \quad \ldots (93)$$

They have proved that this family of functions is non-differentiable at a countable infinite set of points for $\beta > \frac{3}{4}$. Making reference to work of the above authors, we simply state a few results that are needed to study the properties of non-differentiability of W_β.

A direct computation leads us to the following space-scale representation of $W_\beta(t)$ as

$$W_\beta(t) = \int_0^a \frac{da}{a} \int_{-\infty}^{\infty} \frac{1}{a} h\left(\frac{t-b}{a}\right) \theta(\tau) db \quad \ldots (94)$$

where $\tau = b + ia$, $\theta(\tau) = (Im\tau)^\beta \vartheta(\tau)$ and $\vartheta(\tau)$ is a Jacobi theta function defined by

$$\vartheta(\tau) = 1 + \frac{1}{2} \sum_{n=1}^{\infty} \exp(i\pi \tau n^2), \quad Im(\tau) > 0, \quad \ldots (95)$$

and h is any integrable function that satisfies the condition

$$\int_0^a \frac{1}{a}\hat{h}(a)a^{\beta}e^{-a}da = 1, \text{ and } \quad \hat{h}(0) = 0. \qquad \ldots (96)$$

This analysis indicates that the local behaviour of W_β is transformed into that of analytic functions near the boundary of its domain of analyticity. The main conclusion of this discussion is that wavelet transform analysis can be used successfully to prove non-differentiability of both the Weierstrass and Riemann functions.

However, more recently, Jaffard[43] alone and in collaboration with Meyer[16] made a more precise description of the behaviour of W. His analysis focused on the irrational points of the Riemann function which has been a major test functions for wavelets in microlocal analysis.

8 Applications to the Study of Distant Galaxies

The large-scale distribution of galaxies in the Universe reveals various structures at different scales. There are groups, clusters and superclusters of galaxies. The clusters of galaxies include three main components: galaxies, an intracluster medium made of hot gases radiating in the X-ray window, and an amount of dark matter. The baryonic matter is essentially in the form of ionized hydrogen which is found in images obtained in the X-ray bands with satellites. Sub-clusters have also been found in many clusters and their study is of great interest in describing the dynamical state of the clusters of galaxies. Multiscale methods based on the wavelet transform are employed to quantify these sub-clusters. Counts of galaxies play an important role in studying the distant Universe. These counts are determined by using the so called *vision model* based on the wavelet transform analysis. The reference image exhibiting a set of faint galaxies is also obtained. This led to an inventory procedure for large astronomical images. Large scale structures from galaxy counts have been detected. The complex distribution of galaxies and of a cluster of galaxies is now known up to scales of 50 Mpc^2 with a Hubble constant, 100 Km/s/Mpc. The major feature of the galaxy distribution is the deviation from homogeneity at all scales within reach. The topological features of the distribution are characterized by complex structures, one-dimensional filaments or two-dimensional sheets. The high density structures seem to relate clusters of galaxies and to delineate large spherical domains which are free from bright galaxies. Recent studies suggest that the wavelet transforms provide a space-scale analysis in which under- or overdense structures are determined according to their typical size.

In order to determine different structures, cluster algorithms are employed to find out the galaxy counts. However, these algorithms have various limitations in determining the galaxy organization. Based on the assumption that galaxies are distributed according to a Poisson process with a nonuniform density distribution, image processing analysis, known as the vision model, is used with a single spatial scale. Subsequently, the multiscale vision model is also developed. Since the structures of galaxies are more or less hierarchically organized, specific vision models are developed in order to determine, describe and classify each component of the hierarchical organization of distant objects. A multiscale vision model is found to be very useful to detect structures of different sizes. A discrete wavelet transform analysis is also developed by a trous algorithm. For one-dimensional algorithm, the sampled data are regarded as the inner product of the image function f and the translated scaling function ϕ so that

$$c(0, k) = (f(x), \phi(x-k)). \qquad \ldots (97)$$

We consider the inner products at the scale i given by

$$c(i, k) = \frac{1}{2^i} f\left(f(x), \phi\left(\frac{x-k}{2^i}\right)\right). \qquad \ldots (98)$$

If ϕ satisfies the dilation equation

$$\frac{1}{2}\phi\left(\frac{x}{2}\right) = \sum_n h(n)\phi(x-n), \qquad \ldots (99)$$

then $c(i, k)$ can be iteratively calculated from the relation

$$c(i,k) = \sum_n h(n)c\left(i-1, k+2^{i-1}n\right). \qquad \ldots (100)$$

Using the cubic central B-spline with

$$h(n) = \left\{\frac{1}{16}; \frac{1}{4}; \frac{3}{8}; \frac{1}{4}; \frac{1}{16}\right\}, \quad |n| \le 2, \qquad \ldots (101)$$

we employ the wavelet originating from the difference between two successive approximations

$$\omega(i,k) = c(i-1, k) - c(i,k). \qquad \ldots (102)$$

Finally, a reconstruction algorithm is obtained by superposing all wavelet images with the smoothest one. The n-dimensional algorithm can be developed with separable B-splines for the successive approximations. Since the $B_3(x)$ is very close to a Gaussian distribution, results correspond to quasi-isotropic in nature.

Recently, several authors have discussed some applications of astrophysical data of cosmological interest. The analysis of n-body simulations reveals that the vision model based on the wavelet transform provides a new statistical information on cosmological problems. In order to obtain more detailed discussion of this section, the reader is referred to papers by Slezak *et al.*[44,45], Mallat[13], de Lapparent *et al.*[46], Giovanelli *et al.*[47], Huchra *et al.*[48], Bahcall[49], Escalera and Mazure[50] and Escalera[51].

9 Applications of Wavelet Analysis to Turbulence

With the advent of supercomputers, considerable progress has been made on turbulence research based on numerical methods for the last twenty years. Several authors including Ashurst *et al.*[52], Vincent and Meneguzzi[53,54] have developed high resolution direct numerical simulations (DNS) to study the importance and role of coherent structures (vortices and vortex tubes) in three-dimensional turbulent flows. DNS are essentially concerned with numerical solutions of the Navier-Stokes equations. These DNS schemes currently in use can be classified into three categories: (i) finite-difference methods, (ii) spectral and pseudo-spectral schemes and Lagrangian methods (vortex methods). However, they can only deal with simple geometrical configurations and *moderate* Reynolds numbers. In spite of this progress, turbulence modelling is still extremely complex due to lack of knowledge of the intrinsic dynamics of turbulent flows.

On the other hand, several authors including Farge *et al.*[55-60], Meneveau[61], and Fröhlich and Schneider[62,63] developed wavelet analysis to investigate the structure and dynamics of turbulent flows. These studies reveal that the strongest modes of the wavelet transform of two-dimensional turbulent flows represent the coherent structures, while weaker modes describe the unorganized background flow. Furthermore, the study of Wickerhauser *et al.*[64] shows that coherent vortices can be well described by only a very few wavelet modes. Since the dynamics of turbulent flows are largely controlled by their coherent structures, the above studies suggest that wavelet analysis could be an effective method for an accurate and deeper understanding of turbulent flows.

The dynamics of turbulent flows depends not only on different length scales, but on different positions and directions. Consequently, physical quantities such as energy, vorticity, enstrophy and pressure become highly intermittent. The Fourier transform analysis cannot give the local description of turbulent flows, but the wavelet transform analysis has the ability to provide a wide variety of local information of the physical quantities associated with turbulence[28]. So the wavelet transform is adopted to define the space-scale energy density by

$$\tilde{E}(l,x)=\frac{1}{l}\left|\tilde{f}(l,x)\right|^2, \qquad \ldots(103)$$

where $\tilde{f}(l,x)$ is the wavelet transform of a given function (or signal) $f(x)$.

It is natural to introduce a *local energy spectrum* $\tilde{E}(l,x_0)$ in the neighbourhood of x_0[58] by

$$\tilde{E}_x(l,x_0)=\frac{1}{l}\int_{-\infty}^{\infty}\tilde{E}(l,x)\chi\left(\frac{x-x_0}{l}\right)dx, \qquad \ldots(104)$$

where the function χ is considered as a filter around x_0. In particular, if χ is a Dirac delta function, then the local wavelet energy spectrum becomes

$$\tilde{E}(l,x_0)=\frac{1}{l}\left|\tilde{f}(l,x_0)\right|^2. \qquad \ldots(105)$$

The *local energy density* can be defined by

$$\tilde{E}(x)=C_\psi^{-1}\int_{-\infty}^{\infty}\tilde{E}(l,x)\frac{dl}{l}. \qquad \ldots(106)$$

On the other hand, the *global wavelet spectrum* is given by

$$\tilde{E}(l)=\int_{-\infty}^{\infty}\tilde{E}(l,x)dx. \qquad \ldots(107)$$

This can be expressed in terms of the Fourier energy spectrum $\hat{E}(k)=\left|\hat{f}(k)\right|^2$ so that

$$\tilde{E}(l)=\int_{-\infty}^{\infty}\tilde{E}(k)\left|\hat{\psi}(lk)\right|^2 dk, \qquad \ldots(108)$$

where $\hat{\psi}(lk)$ is the Fourier transform of the analyzing wavelet ψ. Thus the global wavelet energy spectrum corresponds to the Fourier energy spectrum smoothed by the wavelet spectrum at each scale.

Another significant feature of turbulence is the so called *intermittency phenomenon*. Farge *et al.*[56,57] used the wavelet transform to define the *local intermittency* as the ratio of the local energy density and the space averaged energy density in the form

$$I(l,x_0)=\frac{\left|\tilde{f}(l,x_0)\right|^2}{\left\langle\left\langle\left|\tilde{f}(l,x)\right|^2\right\rangle\right\rangle}, \qquad \ldots(109)$$

where

$$\left\langle\left\langle\left|\tilde{f}(l,x)\right|^2\right\rangle\right\rangle=\int_{-\infty}^{\infty}\left|\tilde{f}(l,x)\right|^2 dx. \qquad \ldots(110)$$

If $I(l, x_0)=1$ for all l and x_0, then there is no intermittency, that is, the flow has the same energy spectrum everywhere, which then corresponds to the Fourier energy spectrum. According to Farge *et al.*[56,57], if $I(l, x_0)=10$, the point at x_0 contributes ten times more than average to the Fourier energy spectrum at scale l. This shows a striking contrast with the Fourier transform analysis which can describe a signal in terms of wavenumbers only, but cannot give any local information. Several authors including Farge and Rabreau[65], Farge[58], Meneveau[66] have employed wavelets to study homogeneous turbulent flows in different configurations. They showed that during the flow evolution, beginning from a random vorticity distribution with a k^{-3} energy spectrum, the small scales of the vorticity become increasingly localized in physical space. Their analysis also revealed that the energy in the two-dimensional turbulence is highly intermittent which may be due to a condensation of vorticity field into vortex-like coherent structures. They have also found that the smallest scales of the vorticity are confined within vortex cores. According to Farge and Holschneider[67,68], there exist quasi-singular coherent structures in two-dimensional turbulent flows. These kinds of structures are produced by the condensation of vorticity around the quasi-singularities already present in the initial data. Using the wavelet transform analysis, Meneveau[61] first measured the local energy spectra and then carried out direct numerical simulations of turbulent shear flows. His study reveals that the mean spatial values of the turbulent shear flow agree with their corresponding results in Fourier space, but their spatial variations at each scale is found to be very large, showing non-Gaussian statistics. Moreover, the local energy flux associated with very small scales exhibits large spatial intermittency. His computational analysis of the spatial fluctuations of $T(k, t)$ shows that the average value of $T(k, t)$ is positive for all small scales and negative for large scales indicating the transfer of energy from large scales to small scales so that energy is eventually dissipated by viscosity. This finding agrees with the classical cascade model of three-dimensional turbulence. However, there is a striking new phenomenon, that is, the energy cascade is reversed in the sense that energy transfer takes place from small to large scales in many places in the flow field. Recent work of Perrier *et al.*[69] confirms that the mean wavelet spectrum $\tilde{E}(k)$ is given by

$$\tilde{E}(k)=\int_0^{\infty}\tilde{E}(x,k)dx. \qquad \ldots(111)$$

This result gives the correct Fourier exponent for a power-law of the Fourier energy spectrum $E(k)=Ck^{-p}$ provided the associated wavelet has at least $n>\frac{1}{2}(p-1)$ vanishing moments. This condition is in agreement with that for determining cusp singularities. Based on a recent wavelet analysis of a numerically calculated two-dimensional homogeneous turbulent flow, Benzi and Vergassola[70] confirmed the existence of coherent structures with negative exponents. So their study reveals that the wavelet transform analysis has the ability not only to give more precise local description, but also to determine and characterize singularities of turbulent flows. On the other hand, Argoul *et al.*[71,73] and Everson *et al.*[74] have done considerable research on turbulent flows using wavelet analysis. They showed that the wavelet analysis has the ability to reveal Cantor like fractal structure of the Richardson cascade of turbulent eddies.

We close this section by adding some recent and

new development of two-dimensional turbulence based on adaptive wavelet analysis (see Fröhlich and Schneider[62,63], Schneider[75,76]). The unsteady motion of an incompressible viscous fluid flow is described by the Navier-Stokes equations and the continuity equation. In the absence of an external force field, the Navier-Stokes equations and the continuity equation for the two-dimensional flow $((\omega.\nabla)\mathbf{u}=0)$ can be formulated in terms of the velocity and forticity field $\omega=\nabla\times\mathbf{u}=0)$ can be formulated in terms of the velocity and vorticity field $\omega=\Delta\times\mathbf{u}$ in the form

$$\frac{\partial\omega}{\partial t}+(\mathbf{u}\cdot\nabla)\,\omega=\nu\nabla^2\omega, \qquad \ldots(112)$$

$$div\ \mathbf{u}=0, \qquad \ldots(113)$$

where $\mathbf{u}=(u,\ v)$ is the velocity field and ν is the kinematic viscosity of the fluid. This system can be completed by adding appropriate boundary and initial data.

The kinematic energy of the system is given by

$$E(t)=\frac{1}{2}\int\int_D \mathbf{u}^2(\mathbf{x},t)\,d\mathbf{x}, \qquad \ldots(114)$$

where $\mathbf{x}=(x,\ y)$, and the enstrophy is

$$Z(t)=\frac{1}{2}\int\int_D \omega^2(\mathbf{x},t)\,d\mathbf{x}. \qquad \ldots(115)$$

The energy dissipation and the enstrophy are related by the following equations

$$\frac{dE}{dt}=-2\nu E \quad\text{and}\quad \frac{dZ}{dt}=-2\nu P, \qquad \ldots(116a,b)$$

where

$$P(t)=\frac{1}{2}\int\int_D |\nabla\omega|^2\,d\mathbf{x} \qquad \ldots(117)$$

represents the *palinstrophy*.

The associated energy spectrum and the enstrophy spectrum are given by

$$E(k)=\frac{1}{2}\sum_{k-\frac{1}{2}<|\mathbf{k}|\le k+\frac{1}{2}}\left|\hat{u}(\mathbf{k})\right|^2,$$

$$Z(k)=\frac{1}{2}\sum_{k-\frac{1}{2}<|\mathbf{k}|\le k+\frac{1}{2}}\left|\hat{\omega}(k)\right|^2, \qquad \ldots(118)$$

where $\mathbf{k}=(k_1,\ k_2)$ and $|\mathbf{k}|^2=k^2=(k_1^2+k_2^2)$. The quantities $E(k)$ and $Z(k)$ measure the amount of energy on enstrophy in the range of wavenumbers between k and $k+dk$, and are defined by the Fourier transform

$$\hat{f}(k)=\frac{1}{(2\pi)^2}\int\int_D \exp(-i\mathbf{k}\cdot\mathbf{x})\,f(\mathbf{x})\,d\mathbf{x}. \qquad \ldots(119)$$

The energy and enstrophy spectra are related by the formula $Z(k)=k^2E(k)$.

Schneider *et al.*[75,76] has recently developed an adaptive wavelet analysis for solving the two-dimensional Navier-Stokes equations in the domain of simulation $D=[0,\ 2\pi]\times[0,\ 2\pi]$, that is, a 2π square box with periodic boundary conditions. This method is compared with nonlinear Fourier filtering and nonlinear wavelet filtering at each time step. It is shown that the adaptive wavelet simulation is found to reproduce very accurately the dynamics and vorticity structure of a classic pseudospectral simulation of a highly nonlinear interaction of three vortices in two dimensions. On the other hand, nonlinear wavelet filtering produces less well-localized errors, but loses a significant amount of energy and does not reproduce the flow structure as accurately as the adaptive wavelet simulation method. Moreover, the greater accuracy and reduced number of degrees of freedom of the adaptive wavelet simulation compared with nonlinear wavelet filtering is essentially due to the security zone added around the active coefficients and to the compression of the nonlinear convective term of the Navier-Stokes equations in the wavelet basis. This analysis reveals that nonlinear Fourier filtering of a classical pseudospectral method fails to produce significant improvement, but the adaptive wavelet method produces highly accurate results with fewer active modes. The classical pseudospectral method does not exploit the vortical structure of high Reynolds number flows, but the adaptive wavelet analysis seems to be very efficient for describing the dynamics and structures of turbulent flows at high Reynolds number.

In spite of the above convincing features of the adaptive wavelet analysis to two-dimensional turbulence, it is not easy to apply the method to three-dimensional turbulent flows. The main difficulty is that the Navier-Stokes equations in three-dimensions cannot be reduced to pseudo-scalar equations. However, the compression properties of wavelets make them an encouraging method for DNS of three-dimensional coherent

vortices and the vortex tubes. It remains an open question whether the dynamics of three-dimensional turbulence is controlled by coherent vortices.

10 Other Examples of Applications of Wavelets

In general, signal processing deals with extraction of specific information from a signal $f \in L^2(R)$ such as existence of certain patterns, periodic ranges, regularities, singularities and other similar features. It is generally believed that wavelet transforms have become a powerful tool of nonstationary signals of various kinds such as sound, radar, sonar, seismic, biomedical signals (electrocardiogram, ECG in short) and for image processing, image compression and pattern recognition.

The ECG signal represents the changes in electrical potential during the cardiac cycle as recorded between surface electrodes on the human or animal body. The characteristic feature of the signal is the result of an action potential that propagates within the heart and causes the contraction of the various portions of the cardiac muscle.

Wavelet analysis[77] has been used to characterize beat-to-beat fluctuations of the heart rate under variable physiological conditions. One of the major advantages of this new analysis lies clearly in the splitting up in the original signal on various scales. Different properties of the signal can be studied on different scales. A wavelet analysis of blood pressure signals has also been made by Hammer *et al.*[78]. All recent successes are probably due to time-frequency localization properties of wavelet transforms.

Another area of application of wavelet analysis deals with biomedical image processing algorithms (for example, image enhancement, noise reduction and identification of microcalcifications in mammograms), image construction and acquisition schemes (tomography, and magnetic resonance imaging (MRI)), and multiresolution methods for the analysis of the brain (positron emission tomography). Furthermore, higher dimensional signals that require high quality compression is multispectral imagery as produced by remote sensing[79]. Similarly, tomography or nuclear magnetic resonance (NMR) image processing requires higher dimensional high quality compression analysis. So three-dimensional wavelet or subband coding is a possible scheme for investigation. Wavelet analysis[80] is also employed to study electromagnetic waves, that is, solutions of Maxwell's equations. This seems natural because Maxwell's equations in free space are invariant under a group of symmetries (the *conformal group* of space-time) which includes translations and dilations as they are associated with wavelet transforms. Similar to the electromagnetic wave phenomena, construction of wavelet representations of acoustics is also possible. Wavelet analysis is useful for modelling acoustic scattering and sonar. In addition, electromagnetic wavelets[80,81] are found to be very useful for radar signal analysis and electromagnetic scattering.

Multiresolution signal analysis was first introduced by Burt and Adelson[82,83] for multiscale image decomposition, coding and reconstruction. With the development of the basic algorithms for the fast computation of the discrete wavelet transform, various aspects of image processing have been studied[84] with great success. Special attention has been given to the compression of digital images. Especially, wavelet compression algorithms became successful when the algorithm is applied in three steps involving transformation, quantization and coding[85] with proper tuning and optimization. In recent years, the application of wavelet compression algorithms has drawn more attention than any other application. A new class of coding algorithms developed in recent years has enjoyed significant improved performance over the previous class. The significant feature of this new class is that it exploits the wavelet's space-frequency compaction properties, while the previous one is based on only the frequency compaction properties[86].

11 References

1 J Morlet, G Arens, E Fourgeau and D Giard *J Geophys* **47** (1982a) 203

2 J Morlet, G Arens, E Fourgeau and D Giard *J Geophys* **47** (1982b) 222

3 A Grossmann and J Morlet *SIAM J Math Anal* **15** (1984) 723

4 D Gabor *J Inst Electr Eng London* **93** (1946) 429
5 H S Malvar *IEEE Trans ASSP* **38** (1990a) 969
6 H S Malvar *IEEE Trans Acoust Speech Signal Processing* **38** (1990b) 969
7 Y Meyer *Ondelettes, fonctions splines et analyses gradu'ees*, Lecture Notes University of Torino Italy (1986)
8 I Daubechies, A Grossmann and Y Meyer *J Math Phys* **27** (1986) 1271
9 P G Lemarie and Y Meyer *Revista Mat Iberoamer* **2** (1986) 1
10 S Mallat *Multiresolution Representation Wavelets* Ph D Thesis University of Pennsylvania (1988)
11 S Mallat *Trans Amer Math Soc* **315** (1989a) 69
12 S Mallat *IEEE Trans Patt and Mach Intell* **11** (1989b) 678
13 S Mallat *IEEE Trans Acoust Speech Signal Processing* **37** (1989c) 2091
14 G Battle *Commun Math Phys* **110** (1987) 601
15 P G Lemarié *J Math Pure Appl* **67** (1988) 227
16 Y Meyer *Wavelets, Algorithms and Applications* (Translated by Robert D Ryan) *SIAM* (1993)
17 I Daubechies *Commun Pure Appl Math* **41** (1988) 909
18 R J Duffin and A C Schaeffer *Trans Amer Math Soc* **72** (1952) 341
19 I Daubechies *IEEE Trans Inform Theory* **36** (1990) 961
20 I Daubechies Ten Lectures on Wavelets, CBMS-NSF Regional Conference Series in Applied Math **61** *SIAM* Press Philadelphia (1992)
21 A Cohen, I Daubechies and J Feauveau *Comm Pure appl Math* **45** (1992a) 485
22 A Cohen *Biorthogonal Wavelets* In: *Wavelets. A Tutorial in Theory and Applications* Academic Press (1992b) 123
23 C K Chui and J Z Wang *Proc Amer Math Soc* **113** (1991) 785
24 C K Chui and J Z Wang *Trans Amer Math Soc* **330** (1992) 903
25 G Beylkin, R Coifman and V Rokhlin *Comm Pure appl Math* **44** (1991) 141
26 (*a*) R R Coifman, Y Meyer and M V Wickerhauser *Wavelet analysis and signal processing In*: *Wavelets and Their Application* (*Ed:* Ruskai *et al.*) Jones and Bartlett, Boston (1992a) 153
26 (*b*) R R Coifman, Y Meyer and M V Wickerhauser *Size Properties of Wavelet Packets* Jones and Bartlett Boston (1992b) 453
27 L Debnath *Internat J Math Edu Sci Tech* **29** (1998)
28 L Debnath *Nonlinear Instability Chaos and Turbulence* (*Ed:* L Debnath and D N Riahi) *Computational Mechanics Publications* (1998) 129
29 L Debnath *Integral Transforms and Their Applications* CRC Press Boca Raton Florida (1995)
30 R J Glauber *Quantum Optics and Electronics* (*Ed:* C De Witt, A Blandin and C Cohen-Tannoudji (*Gordon and Breach New York*) (1964)
31 A Zayed *Advances in Shannon's Sampling Theory* CRC Press Boca Raton (1993)
32 J Ville *Cables et Transmissions* **2A** (1948) 61
33 (*a*) A J Janssen *J Math Anal Appl* **80** (1981a) 156
33 (*b*) A J Janssen *J Math Anal Appl* **83** (1981b) 377
34 J Klauder and B S Skagerstam *Coherent States* World Scientific Publications Singapore (1985)
35 E W Aslaksen and J R Klauder *J Math Phys* **9** (1968) 206
36 E W Aslaksen and J R Klauder *J Math Phys* **10** (1969) 2267
37 L Debnath and P Mikusinski *Introduction to Hilbert Spaces with Applications* (Second Edition) Academic Press Boston (1999) *to appear*
38 G Strang *SIAM Review* **31** (1989) 614
39 I Daubechies and J Lagarias *SIAM J Math Anal* **22** (1991) 1388
40 I Daubechies and J Lagarias *SIAM J Math Anal* **23** (1992) 1031
41 M Holschneider *L'analyse d'objects fratals et leur transormate' en Ondolettes, Thes'e* Univ Provensc Marseille (1988)
42 M Holschneider and P Tchamitchian *Invent Math* **105** (1991) 157
43 S Jaffard *The Spectrum of Singularities of Riemann's Function* (Preprint) CERMA ENPC La Courtine (1994)
44 E Slezak, A Bijaoui and G Mars *Astron Astrophys* **227** (1990) 301
45 E Slezak, F Durret and D Gerbal *Astron J* **108** (1994) 1996
46 V de Lapparent, M J Geller and J P Huchra *Astrophys J* **369** (1991) 273
47 R Giovanélli, M Haynes, S T Myers and J Roth *Astron J* **92** (1986) 250
48 J P Huchra, M Davis, D Lathan and J Tonry *Astrophys J Sup Ser* **52** (1983) 89
49 N Bahcall *Ann Rev Astron Astrophys* **26** (1988) 631
50 E Escalera and A Mazure *Astrophys J* **388** (1992)
51 E Escalera *Astrophys J* **423** (1994) 423
52 W T Ashurst, A R Kerstein, R M Kerr and C H Gibson *Phys Fluids* **30** (1987) 2343
53 A Vincent and M Meneguzzi *J Fluid Mech* **225** (1991) 1
54 A Vincent and M Meneguzzi *J Fluid Mech* **258** (1994) 245
55 M Farge and G Rabreau *C R Acad Sci Paris Ser II* **307** (1988) 1479
56 M Farge, M Holschneider and J F Colonna *In Topological Fluid Mechanics* (Ed. A K Moffatt and A Tsinober) Cambridge University Press (1990a) 765
57 M Farge, J Guezenne, C M Ho and C Meneveau *Continuous Wavelet Analysis of Coherent Structures In Studying Turbulence Using Numerical Simulation Databases* (Ed. P Monin, W C Reynolds and J Kim) Centre for Turbulence Research, Stanford, California (1990b) 331
58 M Farge *Ann Rev Fluid Mecha* **24** (1992d) 395
59 M Farge, E Goirand, Y Meyer, F Pascal and M V Wickerhauser *Fluid Dynamics Res* **10** (1992b) 229
60 M Farge, N Kevlahan, V Perrier and E Goirand *Proc IEEE Special Issue on Wavelets* **84** (4) (1996) 639
61 C Meneveau *J Fluid Mech* **232** (1991) 469
62 J Fröhlich and K Schneider *Appl Comput Harmonic Anal* **3** (1996) 393
63 J Fröhlich and K Schneider *Computation of Decaying Turbulence in an Adaptive Wavelet Basis* Preprint SC 96-11 Konrad-Zuse-Zentrum Berlin (1996)

64 M V Wickerhauser, M Farge, E Goirand, E Wesfreid and E Cubillo *Efficiency Comparison of Wavelet Packet and Adapted Local Cosine Basis for Compression of a Two-dimensional Turbulent Field in Wavelets: Theory, Algorithms and Applications* (Ed C K Chui, L Montefusco and L Puccio) Academic Press, Boston (1994) 509

65 M Farge and G Rabreau *Wavelet Transform to Analyze Coherent Structures in Two-dimensional Turbulent Flows Proc Scaling Fractals and Nonlinear Variability in Geophysics I* (1989) Paris

66 C Meneveau *Wavelets Fractals and Fourier Transforms* (Ed. M Farge, J C R Hunt and J C Vassilicos) Oxford Univ Press (1993) 251

67 M Farge and M Holschneider *Two-dimensional Wavelet Analysis of Two-dimensional Turbulent Flow Proc Scaling Fractals and Nonlinear Variability in Geophysics II* (1989) Barcelona

68 M Farge and M Holschneider *Europhys Lett* **15** (1991) 737

69 V Perrier, T Philipovitch and C Basdevant *J Math Phys* **36** (1995) 1506

70 R Benzi and M Vergassola *Fluid Dyn Res* **8** (1991) 117

71 F Argoul, A Arnéodo, J Elezagaray, G Grasseau and R Murenzi *Phys Lett* **A135** (1988) 327

72 F Argoul, A Arnéodo, G Grasseau, Y Gagne, E Hopfinger and U Frisch *Nature* **338** (1989) 51

73 F Argoul, A Arnéodo, J Elezgaray, G Grasseau and R Murenzi *Phys Rev* **A41** (1990) 5537

74 R Everson, L Sirovich and K R Sreenivasan *Phys Lett* **A145** (1990) 314

75 K Schneider and M Farge *C R Acad Sci Paris* **325** (1997) 263

76 K Schneider, N K R Kevlahan and M Farge *Theo Compu Fluid Dynamics* **9** (1997) 191

77 H Tsuji and H Mori *Int J Human-Computer Interaction* **6** (1994) 205

78 H Hammer, P Maab, A Rieder and J U Meyer Abstracts of the 2nd European Conference on Engg and Medicine Stuttgart Germany Elsevier Amsterdam (1993) 322

79 D Tretter and C A Bouman *IEEE Trans Image Process* **4** (1995) 285

80 G Kaiser *Wavelet Electrodynamics; A Short Course 10th Annual Applied Computational Electromagnetics Conference* (1994a)

81 G Kiaser Wavelet Electrodynamics Part II: Atomic Composition of Electromagnetic Waves, Applied and Computational Harmonic Analysis **1** (1994b) 246

82 P Burt and E Adelson *IEEE Trans Comm* **31** (1983a) 482

83 P Burt and E Adelson *ACM Trans on Graphics* **2** (1983b) 217

84 P Maab and H G Stark *Surveys on Mathematics in Industry* **4** (1994) 195

85 B Jähne *Digital Image Processing* Springer Verlag New York (1995)

86 A S Lewis and G Knowles *IEEE Trans Image Process* **1** (1992) 244